Final

Tailings Storage Facility Seepage Modelling

Winu TSF Seepage Modelling, Pilbara region, WA, Australia

Rio Tinto

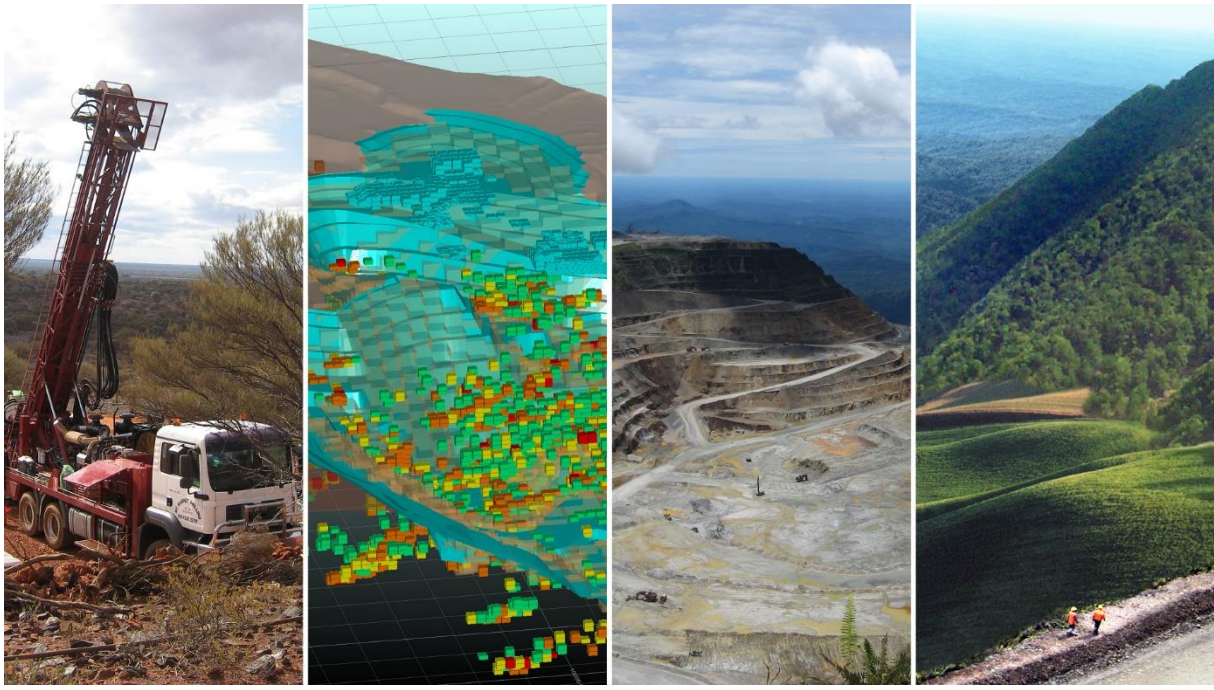

SRK Consulting (Australasia) Pty Ltd ▪ RTS282 ▪ 22 May 2025

srk consulting

Final

Tailings Storage Facility Seepage Modelling

Winu TSF Seepage Modelling, Pilbara region, WA, Australia

Prepared for:
Rio Tinto
Level 9, 152–158 St Georges Terrace
Perth, WA, 6000
Australia

Prepared by:
SRK Consulting (Australasia) Pty Ltd
Level 3, 18–32 Parliament Place
West Perth WA 6005
Australia

+61 8 9288 2000
www.srk.com

ABN: 56 074 271 720

Lead Author: Thomas Robson, PhD **Initials:** TR
Reviewer: Claire Linklater, PhD **Initials:** CL

File Name:
RTS282_Winu TSF Seepage Modelling_Rev2.docx

Suggested Citation:
SRK Consulting (Australasia) Pty Ltd. 2025. Tailings Storage Facility Seepage Modelling. Final. Prepared for Rio Tinto: Perth, WA. Project number: RTS282. Issued 22 May 2025.

srk consulting

Disclaimer: The opinions expressed in this Report have been based on the information supplied to SRK Consulting (Australasia) Pty Ltd (SRK) by Rio Tinto. The opinions in this Report are provided in response to a specific request from Rio Tinto to do so. SRK has exercised all due care in reviewing the supplied information. While SRK has compared key supplied data with expected values, the accuracy of the results and conclusions from the review are entirely reliant on the accuracy and completeness of the supplied data. SRK does not accept responsibility for any errors or omissions in the supplied information and does not accept any consequential liability arising from commercial decisions or actions resulting from them. Opinions presented in this Report apply to the site conditions and features as they existed at the time of SRK's investigations, and those reasonably foreseeable. These opinions do not necessarily apply to conditions and features that may arise after the date of this Report, about which SRK had no prior knowledge nor had the opportunity to evaluate.

Contents

Tables

Figures

Useful Definitions

This list contains definitions of symbols, units, abbreviations, and terminology that may be unfamiliar to the reader.

Abbreviation	Meaning
%	percentage
µS/cm	microsiemens per centimetre
ANC	acid neutralisation capacity
AP	acid potential
BGM	bituminous geomembrane
CO_2	carbon dioxide
D_o	oxygen diffusion coefficient
EC	electrical conductivity
Eq	Equation
g	grams
IOR	intrinsic oxidation rate
kg	kilograms
HST	high sulfur tailings
LOD	limit of detection
LoM	life of mine
LLDPE	linear low-density polyethylene
LST	low sulfur tailings
mg/L	milligrams per litre
NAF	non-acid forming
NAG	net acid generation
NAPP	net acid production potential
NP	net percolation
NPR	neutralisation potential ratio
O_2	oxygen
OCR	oxygen consumption rate
PAF	potentially acid forming
PAF-LC	potentially acid forming – low capacity
PHREEQC	aqueous geochemical speciation modelling code
Project, the	Winu Cu-Au Project (see also *Winu*)
PS	primary sulfides
S	sulfur
SI	saturation index
SRK	SRK Consulting (Australasia) Pty Ltd

Abbreviation	Meaning
SS	secondary sulfides
t	tonnes
TDS	total dissolved solids
TKN	total Kjeldahl nitrogen
TSF	tailings storage facility
UC	uncertain
vol%	volume percentage
WAD	weak acid dissociable
Winu	Winu Cu-Au Project (see also *Project, the*)
WRL	waste rock landform
wt%	weight per cent

Executive Summary

Rio Tinto is proposing to develop the Winu Cu-Au Project (Winu, the Project) in the Pilbara region of Western Australia. Open-pit mining and on-site processing will generate rougher tailings with a low sulfide sulfur content, referred to as low-sulfur tailings (LST), and cleaner tailings with a high sulfide sulfur content, referred to as high-sulfur tailings (HST). Average sulfide sulfur contents for the LST and HST tailings vary from 0.02 wt% to 0.27 wt% and from 0.1 wt% to 22 wt% respectively, depending on ore type. The tailings will be stored in four lined cells (comprised of two LST and two HST cells) in a tailings storage facility (TSF). At closure, covers will be placed to promote saturation of the HST cells and to control dust emissions and erosion of the LST cells. Groundwater affected by TSF seepage is expected to report to the pit lake (a terminal hydraulic sink). A pit lake water quality model has been developed for Winu to project lake water composition for up to 300 years post closure.

The aim of this assessment was to develop a conceptual basis for evaluating if TSF seepage could materially influence future pit lake water quality. To address this objective, SRK evaluated (i) geochemical processes influencing trends in tailings seepage quality, (ii) water flow through the TSF as a function of cover and basal liner performance, and (iii) potential solute transport timeframes and mixing with groundwater between the base of the TSF and the pit lake.

Slow rates of rainwater infiltration and seepage from the TSF suggest that extremely long timeframes (many centuries, even millennia) would elapse before seepage would reach and mix with the underlying groundwater. Initial phases of seepage will resemble process water, which is expected to be near neutral in pH, with dissolved concentrations of some metal(loid)s that could be slightly elevated compared to typical groundwater. The duration of the initial phase could be expected to reflect that of 1–2 tailings pore volume exchanges, which is also in the order of centuries to millennia.

Secondary phases of seepage would be more strongly influenced by oxidation of sulfides present in unsaturated tailings. For HST, the closure designs are expected to limit the rates of tailings desaturation, containing oxidation to thin unsaturated layers near the cover interface over the very long term (many millennia). The LST cells will be partially drained after closure, after which oxidation related processes will influence seepage composition.

Groundwater flux within superficial aquifers beneath the TSF (i.e. perched water tables) is low and, when compared to potential seepage fluxes from the large TSF footprint, may offer limited dilution capacity. Potential long-term influences on groundwater quality in the case of LST were assessed by modelling basal seepage composition, accounting for rates of sulfide oxidation, concomitant solute release, water-mineral interactions and elution from the tailings bed.

The modelling showed that (i) solute release profiles were strongly affected by the relationship between rates of sulfide oxidation (and solute production) and assumed net percolation, (ii) circumneutral pH conditions are expected based on the overall acid-base balance within the tailings solids, and (iii) mineral solubility controls would place upper bounds on seepage concentrations of parameters including sulfate, Al, Ba, Cu, Fe, Mn, Pb, and Zn.

In summary, slow rates of percolation through tailings and underlying strata, combined with low groundwater flux, indicate that seepage would not reach the pit lake for many centuries to millennia.

1 Introduction

The proposed Winu Cu-Au Project is located approximately 300 km south of Broome and 320 km east of Port Hedland in the northern Pilbara region of Western Australia. The proposed (TSF and a waste rock landform (WRL) will be located to the northwest of the mine pit (Figure 1.1). The pit will form a terminal sink in the local hydrogeological environment and a pit lake is expected to form after mining is completed and dewatering operations stop. Seepage from the TSF is expected to report to the pit lake.

Rio Tinto has engaged SRK Consulting (Australasia) Pty Ltd (SRK) to develop a conceptual basis for evaluating if TSF seepage could materially influence future pit lake water quality. To address this objective, SRK evaluated the following:

- geochemical processes influencing trends in tailings seepage quality
- water flow through the TSF as a function of cover and basal liner performance
- potential solute transport timeframes and mixing with groundwater between the base of the TSF and the pit lake.

The geochemical and hydrological processes described herein may occur over prolonged timescales, which are qualitatively referred to as ‘short to medium term’ (within 300 years of closure) and ‘long term’ (order of hundreds to thousands of years).

This report documents the findings from the initial data review, describes the conceptual model used to guide water quality predictions, and presents key model outputs and a high-level impact assessment.

Figure 1.1: Winu tailings storage facility design and location relative to pit void

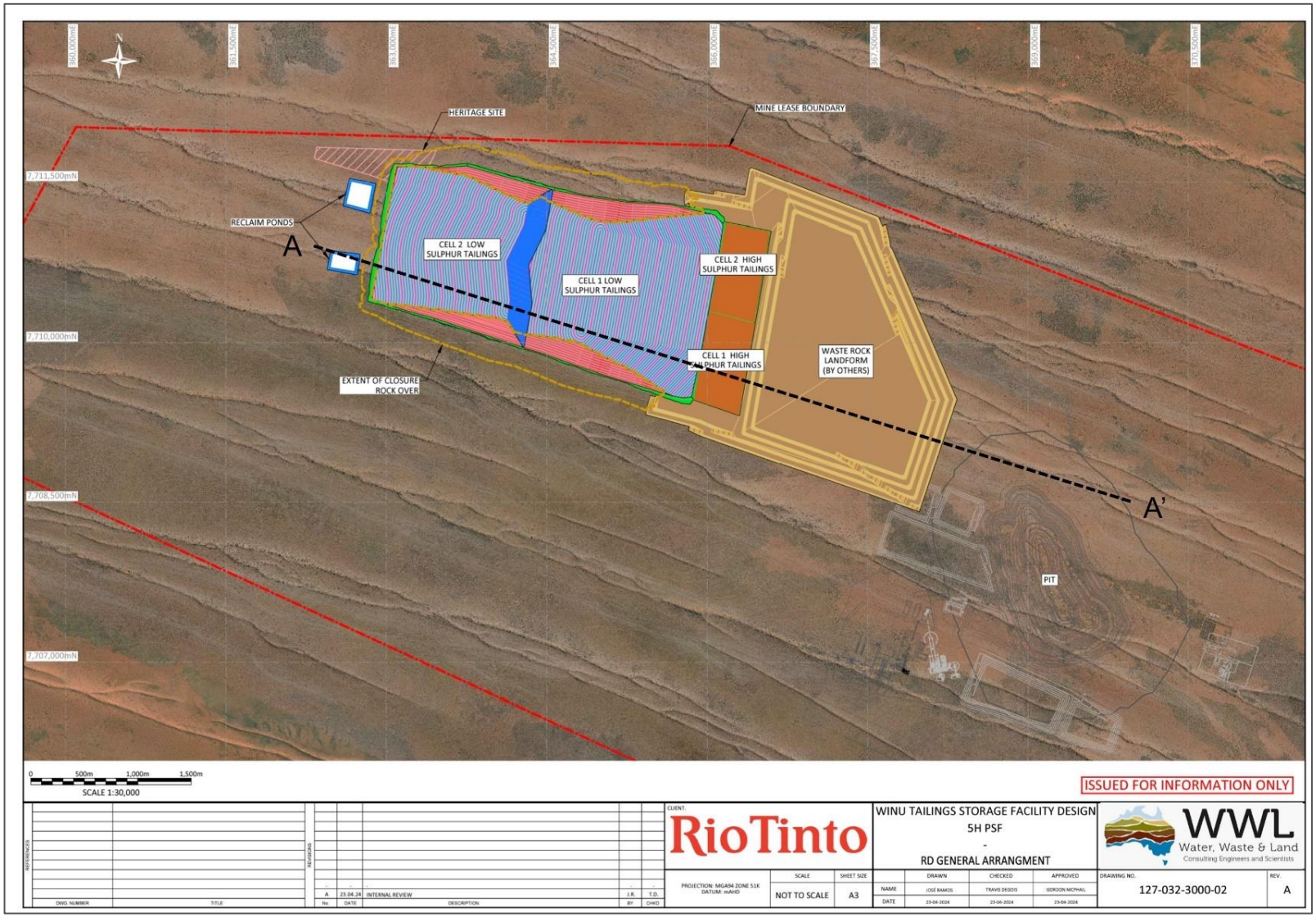

Source: WWL (2024a)

2 Background

2.1 Site setting

2.1.1 Climate

The climate is dry with occasional intense rainfall usually between December and April. Key historical baseline climate parameters are summarised in Table 2.1, as reported by O'Kane (2024). Additional climate data are included in the Winu draft Mine Closure Plan (Rio Tinto, 2024a). Climate change projections from the baseline conditions were incorporated into this assessment, as described in Section 3.2.4.

Table 2.1: Key climate parameters – historical data (1991–2023)

Parameter	Value
Mean annual rainfall	483 mm/yr
Potential evapotranspiration	1,960 mm/yr
Average maximum and minimum temperature in January	38°C and 26°C
Average maximum and minimum temperature in July	27°C and 11°C

Source: O'Kane (2024)
Notes: Based on gridded data from SILO dataset.

2.1.2 Local geology and hydrogeology

Worley Limited (2024a, 2024b) documented a hydrogeological assessment and associated modelling. Hydrogeological modelling has also been completed to support planning for dewatering and water supply for the Winu Project (Advisian, 2022). The information below is largely summarised from these references.

The local topography is relatively flat with low lying sand dunes (west-northwest to east-southeast orientation), typically 5–10 m high and 30–50 m wide. There are occasional clay pans interpreted by Worley to be surface expressions of localised, ephemeral, perched water tables following high rainfall events.

The near surface sands (referred to as 'Aeolian sands' in Figure 2.1 and 'Quaternary aeolian sands' in Table 2.2) are immediately underlain by sandstones (referred to as 'Permian sandstone' in Figure 2.1 and Table 2.2, and referred to hereafter as 'sandstone') and silcrete (10–30 m thick). Below this is a sequence of Permian mudstone, up to 500 m thick in the west of the project area but absent in the eastern portions of the project area. Beneath the TSF, the mudstone can be up to 300 m thick (Figure 2.1).

The deepest rock comprises Proterozoic metasediment that has been subjected to intrusion by mafic dykes. Larger granitic intrusions also exist in the region.

The Project area is located along the eastern margin of the Anketell Fault (Worley, 2024b). The Anketell Fault forms a structural boundary between the Anketell Shelf and the Barnicarndy Graben immediately to the west.

The geological and lithological profiles in the Winu area are illustrated in Figure 2.1 which also presents the hydrostratigraphic units as described in Table 2.2. Conceptual cross sections are shown in Figure 2.2.

Figure 2.1: Geological, lithological and hydrostratigraphic units at Winu

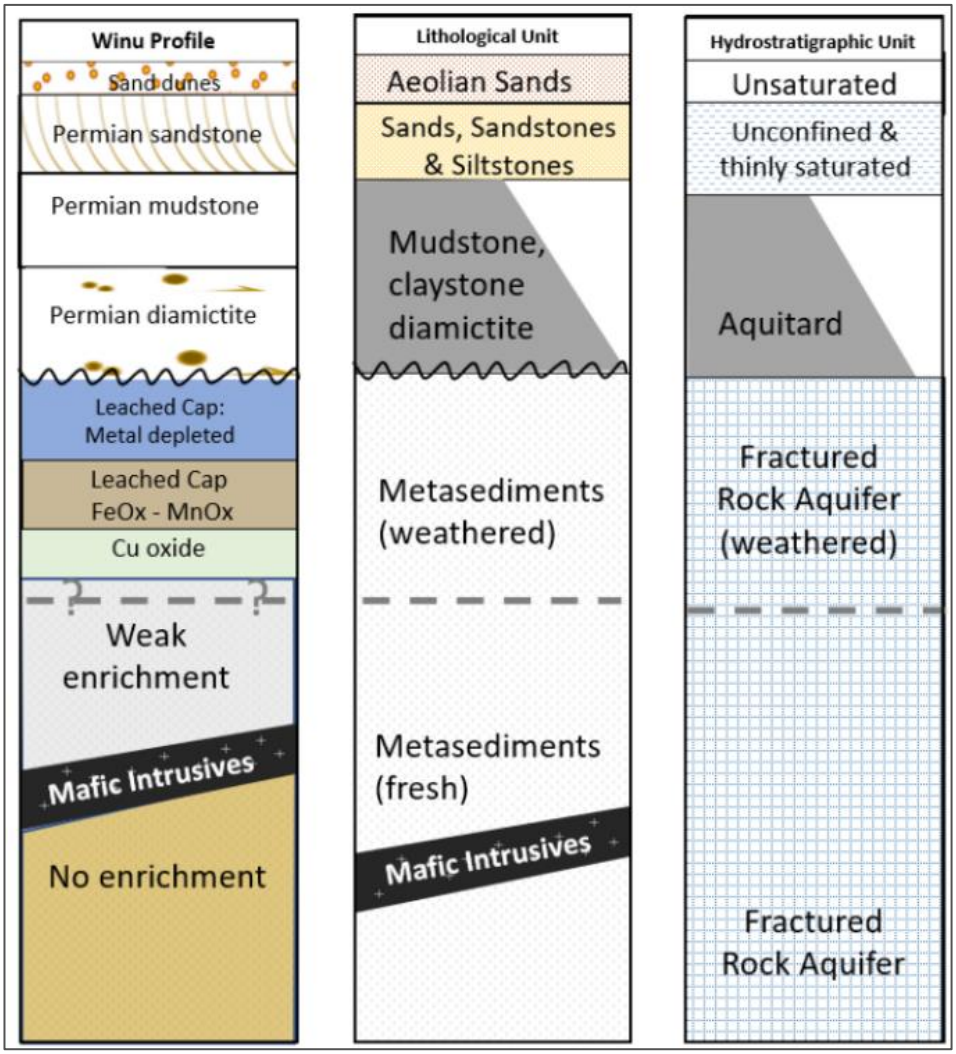

Source: Advisian (2022)

The very near surface units are largely unsaturated, but groundwater may be encountered near the base of the sandstone unit (immediately above the Permian mudstone). The Permian mudstone has a low permeability and is considered an aquitard. The main aquifer in the area is within the Proterozoic metasediment, hosted by fractures and secondary porosity related to weathering, fracturing and faulting. Where the mudstone is absent, there may be connectivity between the fractured metasediment aquifer and the overlying sandstone aquifer (IGS, 2021 – referred to in Worley, 2024b).

The mafic intrusives, where encountered, have low permeability and are expected to inhibit groundwater flow, possibly resulting in compartmentalisation. Pre-mining regional groundwater flow directions were interpreted to be towards the northwest, and the low hydraulic gradient (0.0016, Worley, 2024b) suggests that flow would be slow.

Table 2.2: Hydrostratigraphic units recognised in the Winu area

Hydrostratigraphic unit	Lithology	Thickness (m)	Hydrogeological function	Description
Quaternary aeolian sand	Silty sand, very fine to medium grained	0–10	Unsaturated	Occurs over majority of the study area, unsaturated except following periods of increased rainfall
Silcrete/ferricrete	Silcretised sandstone with variable ferricrete	10–20	Unsaturated	Occurs over majority of the study area, unsaturated
Permian sandstone	Fine to medium grained sandstone	20–50	Unconfined sedimentary aquifer	Variable spatial coverage and thickness, partially saturated
Permian mudstone	Mudstone, claystone, diamictite	0–250	Sedimentary aquitard	Discontinuous, low permeability confining unit
Mafic intrusions	Slightly weathered to fresh, hornblende phenocrysts, micaceous/schistose in some intervals	5–40	Intrusive aquitard	These are interpreted to function as a low permeability facies and presumably inhibit groundwater flow in the metasediment aquifer
Proterozoic metasediment	Moderately to highly weathered metasediment	20–80	Fractured aquifer	Divided into different zones due to faulting and weathering The fresh and weathered zones are inferred to act as a fractured aquifer.
	Slightly weathered to fresh metasediment, massive, fine to coarse grained	>300		
Granite	Slightly weathered to fresh, granite, generally occurs as quartz, feldspar, and biotite in a matrix	>100	Intrusive aquitard	These are interpreted to function as a low permeability facies and presumably inhibit groundwater flow in the metasediment aquifer

Source: Worley (2024b)

Figure 2.2: Conceptual cross sections through the Winu study area

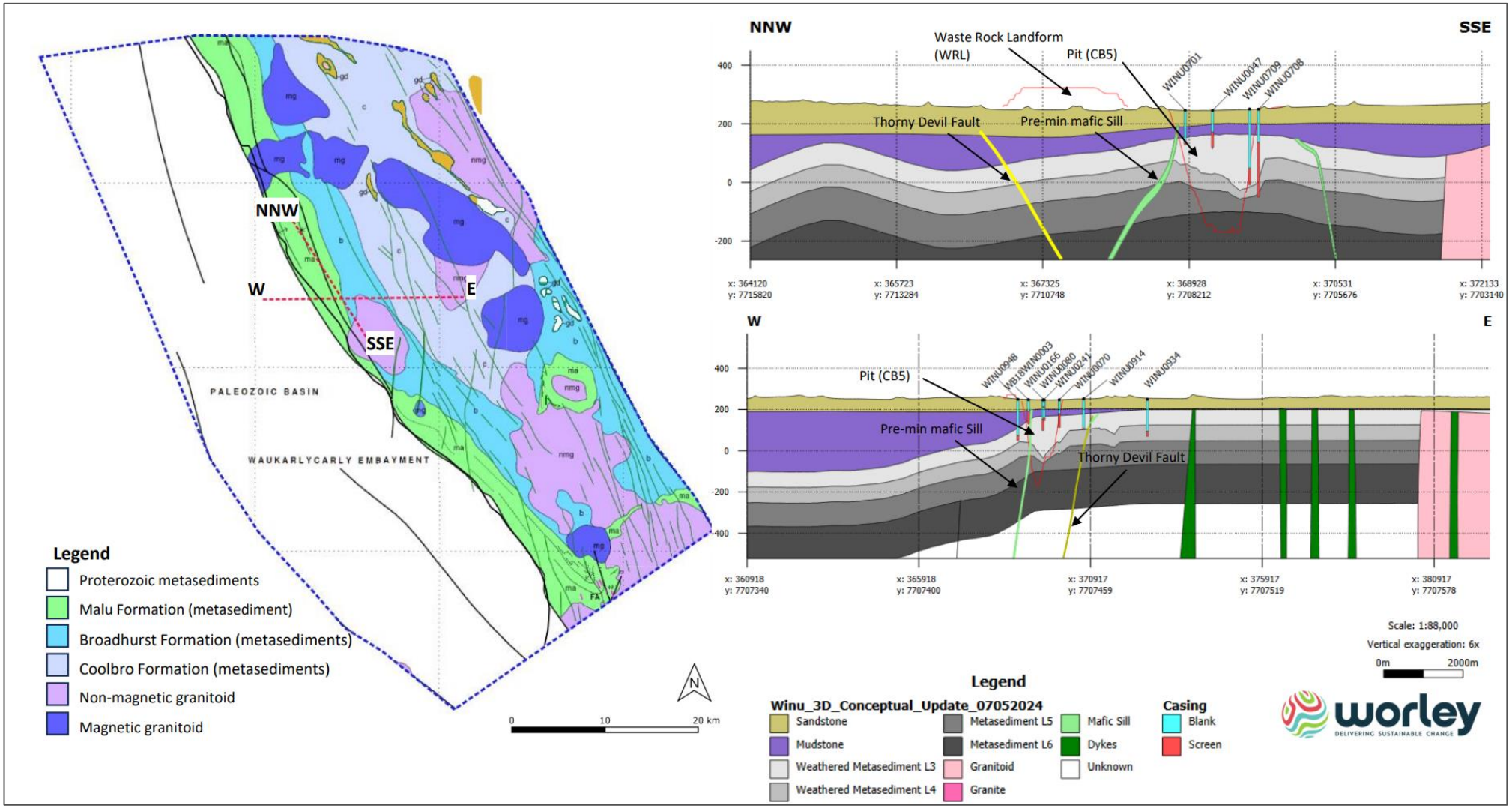

Source: Worley (2024b)

2.2 Groundwater quality

Summary statistics for solute concentrations in bores screened for the sandstone aquifer (described in Section 2.1.2) are presented in Table 2.3. The sandstone aquifer is considered the most relevant for potential TSF seepage transport pathways, as opposed to the Proterozoic metasediment aquifer. While data were not available to summarise groundwater quality in the aeolian sands (i.e. saturated sands overlying silcrete, where present), it is expected to be broadly consistent with the sandstone.

Table 2.3: Summary of groundwater quality in the sandstone aquifer

Parameter	Unit	25th percentile	Average	Median	75th percentile
pH	s.u	7.0	7.5	7.4	7.9
EC (Field)	µS/cm	630	1,200	840	1,500
Total alkalinity	mg/L as $CaCO_3$	73	170	110	260
Ca	mg/L	13	32	17	40
Na	mg/L	70	150	120	200
K	mg/L	7	7.9	8	9
Mg	mg/L	7	9.6	8	10
SO_4	mg/L	17	35	28	43
Cl	mg/L	76	170	120	180
F	mg/L	0.3	0.52	0.5	0.6
Ag	mg/L	*0.00001*	*0.00024*	*0.00001*	*0.00002*
Al	mg/L	*0.01*	0.091	0.03	0.12
As	mg/L	0.002	0.0033	0.003	0.004
B	mg/L	0.24	0.24	0.24	0.26
Ba	mg/L	0.16	0.16	0.16	0.17
Be	mg/L	*0.0001*	*0.0001*	*0.0001*	*0.0001*
Cd	mg/L	*0.0001*	*0.0001*	*0.0001*	*0.0001*
Co	mg/L	*0.0001*	*0.0001*	*0.0001*	*0.0001*
Cr	mg/L	*0.0009*	0.0015	0.001	0.002
Cu	mg/L	*0.002*	0.0065	0.004	0.006
Fe	mg/L	0.09	0.39	0.2	0.4
Li	mg/L	0.0045	0.0049	0.0051	0.0053
Mn	mg/L	0.021	0.31	0.11	0.46
Mo	mg/L	*0.001*	0.01	0.0055	0.012
Ni	mg/L	*0.001*	0.0026	0.002	0.003
Pb	mg/L	*0.0002*	*0.0003*	*0.0003*	*0.0004*
Sb	mg/L	*0.0002*	*0.0002*	*0.0002*	*0.0002*
Se	mg/L	*0.00023*	*0.00025*	*0.00025*	*0.00028*
Si	mg/L	28	28	28	29
Sn	mg/L	*0.0003*	*0.0003*	*0.0003*	*0.0003*
Sr	mg/L	0.27	0.29	0.29	0.31

Parameter	Unit	25th percentile	Average	Median	75th percentile
Tl	mg/L	*0.00002*	*0.00002*	*0.00002*	*0.00002*
U	mg/L	0.00012	0.0002	0.00018	0.00022
V	mg/L	0.00063	0.0022	0.0012	0.0016
Zn	mg/L	0.006	0.03	0.009	0.018

Source: Monitoring database extract provided by Rio Tinto. Data relate to monitoring between November 2020 and November 2024.

Notes: EC – electrical conductivity.

Underlined italics indicate a value strongly influenced by or equal to the limit(s) of detection (LOD) for the dataset. Summary statistics were calculated assuming <LOD values are equal to the LOD.

2.3 Tailings properties and disposal

2.3.1 Metallurgical processing

The proposed metallurgical process comprises crushing and grinding of the ore followed by a gravity gold recovery step. After free gold recovery, the material will be subjected to bulk sulfide flotation to produce a sulfide mineral concentrate and a low-sulfur, rougher tailings product (herein referred to as LST). The sulfide flotation concentrate will be subjected to a secondary flotation step to produce a copper concentrate (final product) and high-sulfur, cleaner tailings (herein referred to as HST).

The LST will be subjected to a carbon-in-leach cyanide extraction step to recover gold. The cyanide leached LST will be detoxified using the sulfur dioxide (SO_2)/air process. The LST will represent 91–95 wt% of the total tailings generated, and the remaining 5–9% will be HST (WWL, 2024a).

2.3.2 Tailings geochemistry

Tailings solid composition

Rio Tinto (2024b) undertook geochemical characterisation of process tailings generated by metallurgical trials on primary/secondary sulfide and oxide ore types, including mineralogy, paste pH/EC, acid-base accounting and net acid generation (NAG) testing, chemical assays and a range of leach testing.

Selected acid-base accounting data summary statistics are presented in Table 2.4. The HST derived from primary and secondary sulfide ore products contain significant sulfur, predominantly as sulfide minerals (pyrite and pyrrhotite) – based on chromium-reducible sulfur testing and mineralogical assessment). ANC is low (<10 kg H_2SO_4/t); mineralogical assessment suggests that the main contributors to ANC may be silicates because carbonate content is low and typically dominated by iron-carbonate (siderite), which is not expected to contribute to pH neutralisation under oxidising conditions. The primary and secondary sulfide ore HST types are classed as potentially acid forming (PAF).

The LST derived from the primary and secondary sulfide ore products also contain sulfur, but at lower levels – 0.27% and 0.22%, respectively – and are classed as PAF with low capacity for acid generation (PAF-LC). Based on life of mine (LoM) modelling, LST will have an average sulfur content of 0.2% (Figure 2.3) (Rio Tinto, 2024b) and – under depositional conditions – are expected to be non-acid forming (NAF). Samples selected for the geochemical characterisation program were biased toward higher sulfur content and not representative of the expected average LST.

Figure 2.3: Life of mine projections for LST sulfur concentration

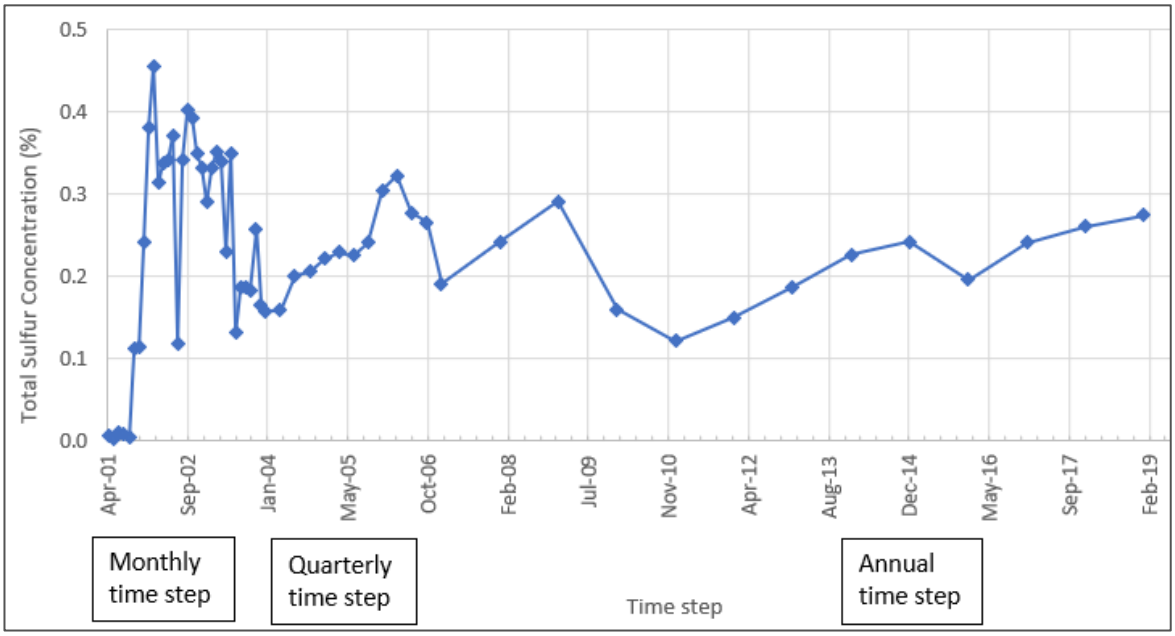

Source: Rio Tinto (2024b)

Note that tailings derived from primary sulfide ore are expected to comprise most (>80%) of the tailings volume, followed by those from secondary sulfide ore. Oxide-derived tailings are expected to be minor (<2% of plant feed) (Rio Tinto, 2024b).

Table 2.4: Selected geochemical properties of LST and HST samples

		Sample count	Average sulfide-S (wt%S)	Average ANC[1] (kg H_2SO_4/t)	NAPP kg (H_2SO_4/t)	NPR	Class
LST	Primary sulfide	29	0.27	9.84	-3.7	2.3	PAF-LC
	Secondary sulfide	6	0.22	4.40	2.3	1.3	PAF-LC
	Primary and secondary sulfides	35	0.20[2]	8.80[3]	-2.6	1.4	-
	Oxide	1	0.02	4.50	-3.9	7.4	NAF
HST	Primary sulfide	11	22.3	6.4	831.4	<0.1	PAF
	Secondary sulfide	3	18.1	5.5	744.2	<0.1	PAF
	Primary and secondary sulfides	14	21.5	6[3]	651	<0.1	-
	Oxide	1	0.1	2.8	-1.3	1.8	NAF

Source: Rio Tinto (2024b)

Notes: NAPP – net acid producing potential; NPR – neutralisation potential ratio; S – sulfur.

[1] ANC dataset comprises customised ANC testing (focused just on ANC from neutralising carbonates) as well as the AMIRA method (including both carbonates and fast reacting silicate minerals). Averages have been calculated using a consolidated dataset where preference is given to the customised method, but where no data are available, the AMIRA data are used.

[2] Projected average sulfide-S content of LST based on LoM expectations (Rio Tinto, 2024b).

[3] Weighted average of ANC based on data presented in Rio Tinto (2024b).

Process water

Table 2.5 lists selected summary statistics calculated from available filtrate data.

Table 2.5: Indicative process water composition (tailings filtrate)

Parameter	Unit	LST filtrate (n=8)			HST filtrate (n=5)		
		Minimum	Average	Maximum	Minimum	Average	Maximum
pH	pH unit	7.9	8.1	8.3	7.4	7.6	8.0
EC	µS/cm	1,070	1,211	1,420	906	1,191	1,380
SO_4	mg/L	42	171	314	44	200	329
Alkalinity	mg/L	74	108	178	21	55	130
Cl	mg/L	213	231	253	230	243	253
F	mg/L	0.9	1.6	2.2	0.5	0.9	1.2
Ca	mg/L	16	44	84	16	55	94
Mg	mg/L	6.0	12.1	18.0	1.0	3.6	7.0
K	mg/L	20	42	53	19	22	26
Na	mg/L	130	149	167	130	164	189
Si	mg/L	5	6	11	3	5	11
Ag	mg/L	*0.0001*	*0.0001*	*0.0001*	*0.0001*	0.0008	0.0018
Al	mg/L	0.03	0.06	0.08	0.04	0.08	0.14
As	mg/L	0.001	0.004	0.010	0.001	0.002	0.007
Au	mg/L	*0.001*	*0.001*	*0.001*	*0.001*	*0.001*	0.003
B	mg/L	0.06	0.117	0.174	0.019	0.075	0.125
Ba	mg/L	0.068	0.124	0.218	0.041	0.095	0.133
Cd	mg/L	0.0001	0.0005	0.0010	0.0001	0.0003	0.0005
Co	mg/L	0.003	0.007	0.012	0.004	0.006	0.010
Cr	mg/L	*0.0002*	0.0003	0.0005	*0.0002*	0.0006	0.0008
Cu	mg/L	0.012	0.071	0.22	0.01	0.51	2.04
Fe	mg/L	*0.002*	0.017	0.063	*0.002*	0.026	0.078
Hg	mg/L	*0.00004*	0.00009	0.00025	*0.00004*	0.00007	0.00014
Mn	mg/L	0.04	0.09	0.15	0.004	0.06	0.09
Mo	mg/L	0.09	0.14	0.17	0.04	0.07	0.10
Ni	mg/L	0.009	0.031	0.051	0.006	0.015	0.022
Pb	mg/L	0.0003	0.0035	0.0109	0.0003	0.0035	0.0092
Sb	mg/L	0.0006	0.0021	0.0030	0.0008	0.003	0.006
Se	mg/L	0.0013	0.0063	0.0116	0.0044	0.014	0.023
Sr	mg/L	0.14	0.30	0.53	0.07	0.15	0.20
Tl	mg/L	0.00013	0.00037	0.00064	0.00011	0.00042	0.00076
U	mg/L	0.0010	0.0021	0.0031	0.00008	0.00064	0.0019
V	mg/L	0.0004	0.0010	0.0018	*0.0002*	0.0010	0.0020
W	mg/L	0.057	0.086	0.133	0.009	0.056	0.113
Zn	mg/L	0.006	0.025	0.051	0.004	0.021	0.041
NO_3_N	mg/L	*0.01*	0.13	0.48	*0.01*	0.14	0.29
NO_2_N	mg/L	*0.01*	0.01	0.01	*0.01*	0.03	0.06
NH_3_N	mg/L	*0.01*	0.03	0.10	*0.01*	0.02	0.04
TKN_N	mg/L	0.1	0.23	0.50	0.2	1.2	5.0
N total	mg/L	0.1	0.35	1.00	0.2	1.4	5.1
Total CN	mg/L	*0.004*	*0.004*	*0.004*	*0.004*	0.32	1.28
Free CN	mg/L	*0.004*	*0.004*	*0.004*	*0.004*	0.16	0.63
WAD CN	mg/L	*0.004*	*0.004*	*0.004*	*0.004*	0.32	1.27

Source: tailings_consolidated_data.xlxs

Notes: TKN – total Kjeldahl nitrogen; WAD – weak acid dissociable.

Underlined italic type indicates a value strongly influenced by or equal to the limit(s) of detection (LOD) for the dataset. Summary statistics were calculated assuming <LOD values are equal to the LOD.

2.3.3 Tailings placement and storage

The following information is summarised from WWL (2024b).

The tailings will be stored in four cells in the TSF (HST Cells 1 and 2, and LST Cells 1 and 2; refer to Figure 2.4). Liners will be placed under all cells. Preferred liner systems comprise a linear low-density polyethylene (LLDPE) liner for the HST cells, due to its chemical resistance and elongation characteristics, and a bituminous geomembrane (BGM) for the LST cells, due to its robustness to accommodate construction activity and lesser need for ground preparation.

Tailings will be deposited into HST Cell 1 and LST Cell 2 approximately for the first 11 years and then into HST Cell 2 and LST Cell 1 for the following 10 years. After this time, deposition will be alternated between HST Cell 1 and HST Cell 2 as well as between LST Cell 1 and LST Cell 2 as closure nears.

The HST cells will be operated with a minimum water depth of 0.5–1 m (1.5 m minimum at the tailings discharge locations – i.e. the HST will be deposited and maintained sub-aqueously to prevent oxidation). These water depths will be maintained when the cells are progressively raised. Evaporation from the water cover will be reduced using evaporation inhibitors (plastic balls).

The low-sulfur cells will be constructed with upstream raises using soil with rockfill backing for closure (Rio Tinto, 2024a). The low-sulfur cells will be equipped with filter drainage over the base liner to promote tailings consolidation and reduce hydraulic head on the liner. Drainage water will drain to a sump from where it will be pumped to the processing plant, along with reclaimed supernatant water.

Two lined reclaim ponds will be constructed to the west of the TSF as an additional water management option. All the TSF cells will be equipped with pumps so that water can be transferred from cell to cell, or to the reclaim ponds, before returning to the processing plant.

2.3.4 Tailings storage facility closure

A dry cover is proposed for final closure of the HST TSF cells. The objective of the proposed cover system is to promote saturation of the HST (Rio Tinto, 2024a). This will be achieved by preventing the upward movement of water from the HST by decoupling the saturated HST from the evapotranspiration zone. Based on cover design modelling studies (O'Kane, 2020, 2024), the cover over the HST may need to be 3–6 m thick. Current designs incorporate a cover comprising at least than 6 m of LST overlain by 0.5 m of NAF metasediment to provide erosion control. The cover design configurations adopted for this assessment are discussed in Section 3.2.4.

It should be noted that the placement of a dry cover would require that the surface of HST tailings be made trafficable for cover construction. To address this requirement while maintaining saturated conditions within the HST tailings, it is proposed that a floating delivery line is positioned over the cells to enable sub-aqueous placement of LST. Once a 2 m cover of LST is placed over the HST, surface water can be drained and the remaining LST cover depth (4 m) can be placed using spigots (WWL, 2024b). The high degree of saturation maintained in the HST will limit oxygen ingress; significant oxidation and acidification should therefore be avoidable in the short to medium term.

The cover over the LST cells is not intended to maintain saturation of the tailings and therefore the cover thickness will likely be 0.5–1 m thick, consisting of NAF metasediment and topsoil to establish vegetation (O'Kane, 2020, 2024; Rio Tinto, 2024a).

Final saturation within the TSF cells is dictated by the water balance; water inflow is controlled by recharge through the cover system while outflows are controlled by leakage through basal liners. Modelling studies have evaluated the long-term conditions within the LST and HST cells (O'Kane, 2020, 2024; WWL, 2024b). Over time, as would be expected, the LST are expected to desaturate to a greater degree than the HST. Current modelling outputs suggest that the HST would be maintained at a high level of saturation (≥85%) over the long term (centuries to millennia). Rates of oxygen diffusion into tailings can be greatly reduced, though not to zero, when saturation exceeds 85% (INAP, 2009).

The TSF design proposes that a filter drainage system will be installed above the liner within LST cells to promote consolidation and reduce hydraulic heads on the basal liner during operations. It is expected that flow through the filter drainage system will continue for 5–10 years after closure while the tailings bed drains down (WWL, 2024b).

Figure 2.4: Proposed layout of TSF at closure

Source: WWL (2024b) Winu TSF Closure Design

Notes: Features shown in blue denote spillway infrastructure for post-closure management of high-intensity rainfall events.

3 Conceptual models

This assessment involved conceptualisation of the key processes and factors expected to influence the geochemistry of tailings porewater and seepage, plus potential transport pathways for seepage-affected groundwater to impact Winu pit lake water quality. The presence of liners is expected to result in negligible seepage during the operational period. Greater focus has therefore been placed on the post-closure period.

3.1 Operational phase

Sulfide oxidation rates are expected to be negligible in the HST cells due to the operational water cover. The oxidation of tailings in the LST cells is expected to be restricted to unsaturated tailings exposed on beaches. Rates of oxidation are expected to be low due to the slow supply of oxygen from the beach surface, as oxygen diffusion would be limited by relatively high moisture saturation during operations.

During operations, seepage quality is expected to resemble process water associated with the respective tailings products (Section 2.3.2). Over time during the operational period, some change in process water chemistry (increasing solute content) could be expected due to evapoconcentration in pond water and the influence of recycling through the process plant.

Seepage during operations would be actively managed. Given the presence of liners beneath the TSF cells, it is expected the basal seepage flux would be very limited and primarily controlled by any imperfections that existed within the liners as constructed. Significant degradation of the liners is not expected to occur during operations.

Based on a basal seepage flux of 0.15 mm/year[1] (0.04% of annual rainfall), any seepage passing through the liners would have percolated downwards only very small distances (a few centimetres) during operational timeframes.

3.2 Post closure

3.2.1 Hydrogeochemical processes

Low sulfur tailings

Much of the process water is expected to drain away in the first 5–10 years post-closure. Residual process water will gradually be displaced by infiltrated meteoric water and in the long term, post-closure seepage quality is expected to be controlled by sulfide oxidation within unsaturated volumes of LST. Among other aspects, the composition of seepage at the base of the TSF is a function of (i) rates of oxidation in unsaturated or partially saturated tailings, (ii) rates of seepage percolation, and (iii) the composition of the tailings solids and those constituents that could react

[1] Based on a study of leakage through holes in geomembranes beneath tailings by Rowe et al. (2016), and adopted by O'Kane Consultants Pty Ltd as the base boundary conditions for the cover system modelling for both LST and HST cells (O'Kane, 2020).

with percolating seepage. These processes are shown in conceptual diagrams for LST Cell 1 (Figure 3.1).

Characterisation results indicate that the LST will comprise NAF and PAF-LC classes but are unlikely to generate significant net acidity under proposed site conditions (Rio Tinto, 2024b). Although the overall acid base account of the mixed LST is marginal (NAPP of -2.6 kg H_2SO_4/t, Table 2.4), additional slow reacting silicate mineral content can be expected to maintain pH neutral conditions within the percolate from the oxidised zone. In the long term, the potential for acidic percolate to be released from the LST is considered unlikely.

Figure 3.1: Conceptual model for seepage quality and transport model (LST cells)

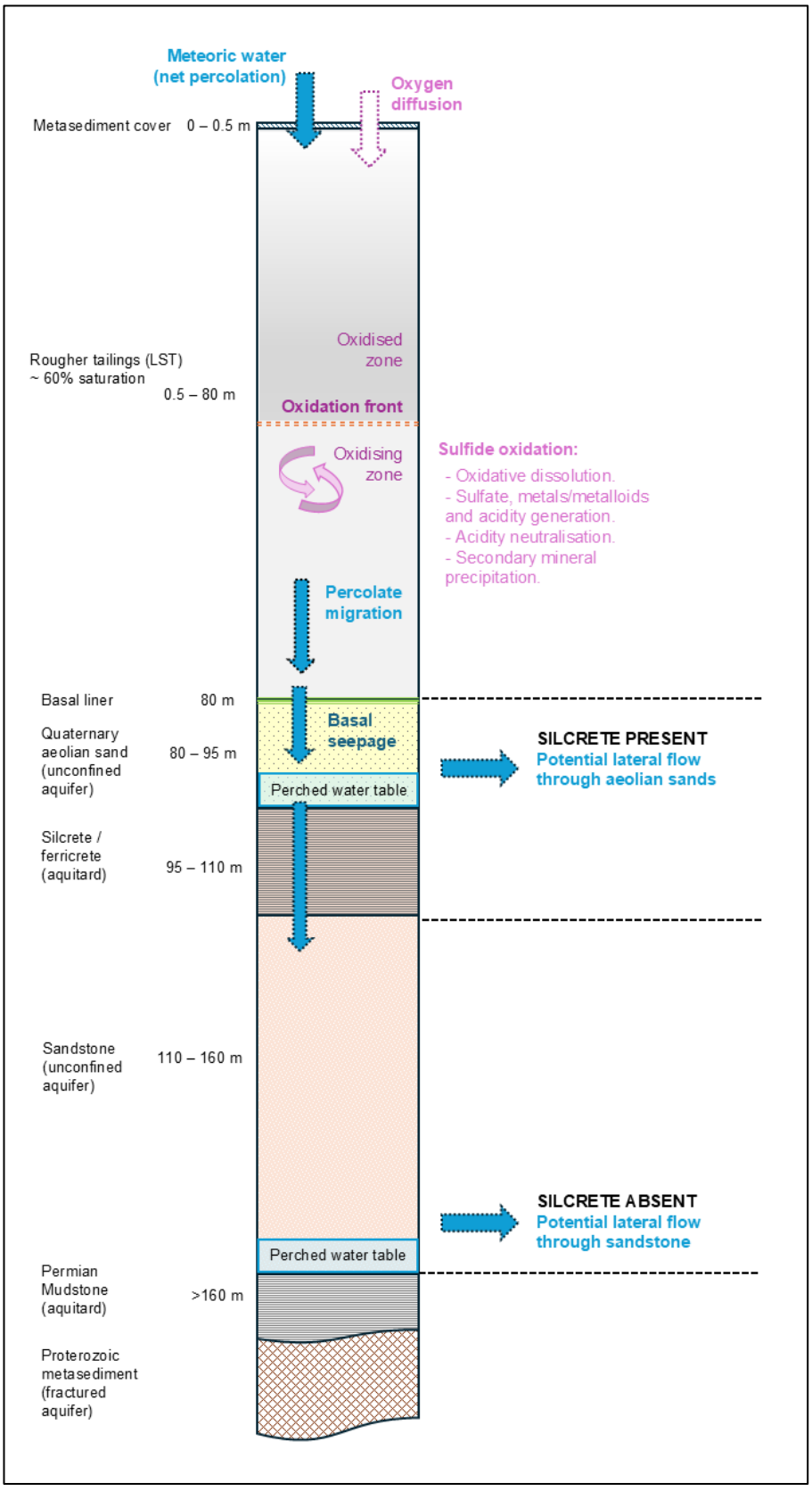

Other processes that could influence seepage quality include development of anoxic or even reducing conditions at depth within the tailings. Some mineral content may be sensitive to redox conditions. Iron and manganese oxides and oxyhydroxides may become more soluble in reducing conditions, leading to increases in dissolved iron and manganese in seepage. Trace elements associated with these minerals may also be released, e.g. nickel and chromium – based on sequential extraction studies reported in Rio Tinto (2024b). Cyanide residues, which are expected to degrade under exposure to environmental conditions, are excluded from this assessment.

High sulfur tailings

The closure strategy for the HST cells is designed to maintain a high degree of saturation within the HST to limit sulfide oxidation. For a range of cover designs, modelling (O'Kane, 2024) has shown that even where the basal liner performance deteriorates over time, the rate of leakage from the HST cells is very slow. Figure 3.2 shows the modelled saturation profiles at 300 years for:

- Base case — Rio Tinto's preferred cover design with a thick layer of LST (6 m), no topsoil layer, basal liner intact
- Worst case — No topsoil layer, basal liner performance has deteriorated.

In both modelled scenarios, the water balance is very slightly negative; therefore, over time, the thickness of the desaturated near-surface zone would increase, albeit very slowly.

Figure 3.2: Minimum degree of saturation versus depth in HST cells at 300 years post closure

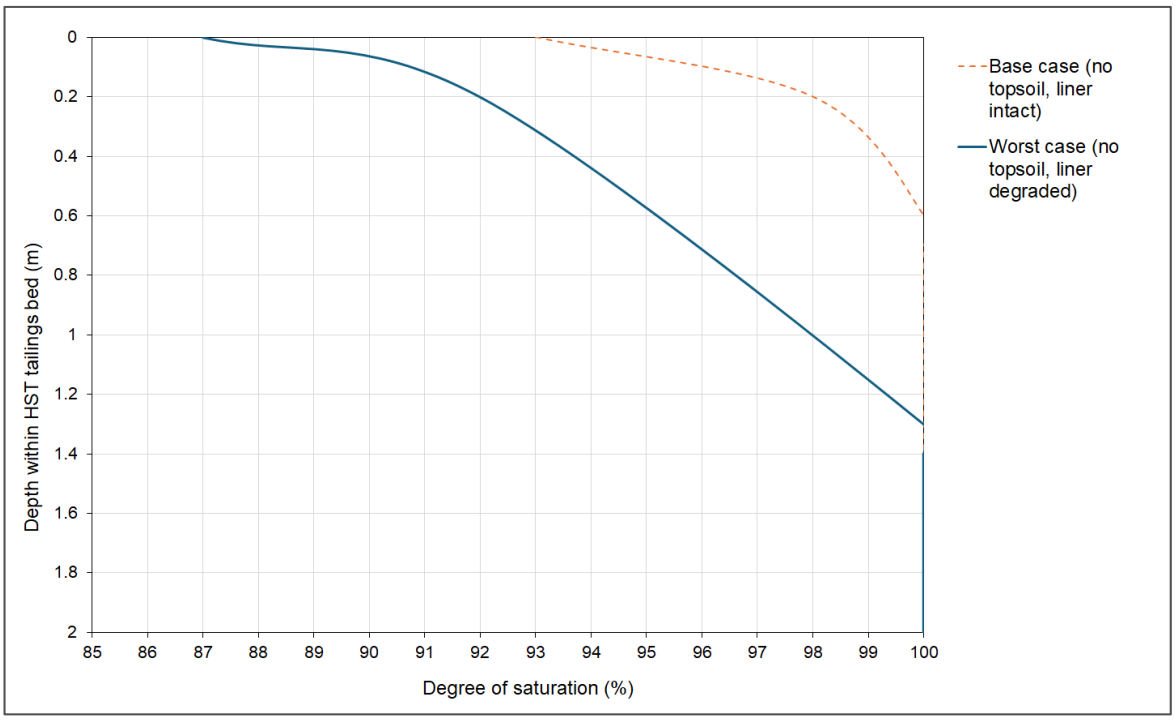

Source: Produced using data from O'Kane (2024)

For the preferred cover design, due to the presence of the overlying LST, the active oxidising zone within the HST may be confined to a very thin layer of unsaturated tailings near the tailings/cover transition – some illustrative calculations (assuming very low diffusivity of oxygen to reflect the high degrees of saturation) suggest the oxidising zone might be of order 0.15 m thick at 300 years post closure. Long timeframes would be necessary to deplete sulfides within this layer given its high sulfide content. This, combined with the slow rate of HST desaturation, means progression of the tailings oxidation front downward would be extremely slow.

3.2.2 Connectivity between TSF and pit

The pit is expected to form a terminal sink in the local hydrogeological system. Figure 3.3 shows predicted groundwater drawdown at the end of mining (Worley, 2024b). Post closure, the groundwater level would rebound and modelling suggests that the final pit lake elevation would remain significantly below the pre-mining groundwater elevation (HydroGeoLogica, 2024). Locally, below the TSF, groundwater flow would be towards the pit.

If low permeability layers are encountered (e.g. clay, silcrete) as seepage percolates downward through underlying strata (refer to Section 2.1.2), then perched water tables may develop and lateral transport of seepage is possible. There is some uncertainty about the distribution and continuity of a silcrete layer beneath the TSF footprint. Should a perched water table develop above the silcrete, lateral flows of this water would be influenced by the topography of the silcrete surface. According to visualisations prepared by Rio Tinto (Figure 3.4), the silcrete layer intersects the pit shell. Lateral transport of seepage along the silcrete surface will report to the upper reaches of the pit wall. Further field work is currently underway to better understand the silcretes and the influence on groundwater flow.

Should seepage pass through the silcrete layer, or where the silcrete is not continuous, it may continue percolating downwards to encounter the sandstone aquifer (some 20–60 m below ground level [m BGL]), which is labelled as ‘shallow aquifer’ on Figure 3.4. As noted for silcrete, it is inferred that a perched water table may form at the base of the sandstone aquifer (labelled as ‘shallow aquifer’ in Figure 3.4). Hydrogeological investigations have indicated that the base of the aquifer is saturated (Worley, 2024b), supporting this inference.

Two conceptual sequences were considered below the TSF, given current uncertainty around the presence and continuity of a silcrete aquitard beneath the proposed TSF location (Table 3.1). A preliminary review of borehole logging suggests that silcrete is present beneath much of the TSF but is not contiguous across the whole proposed footprint, nor in the stretch between the proposed WRL and pit (Figure 3.5). Based on this finding, the sandstone aquifer is considered to be most relevant for transport of seepage-affected groundwater towards the pit. Ongoing hydrogeological investigations by Rio Tinto also support this inference.

Figure 3.3: Predicted groundwater drawdown at the end of mining

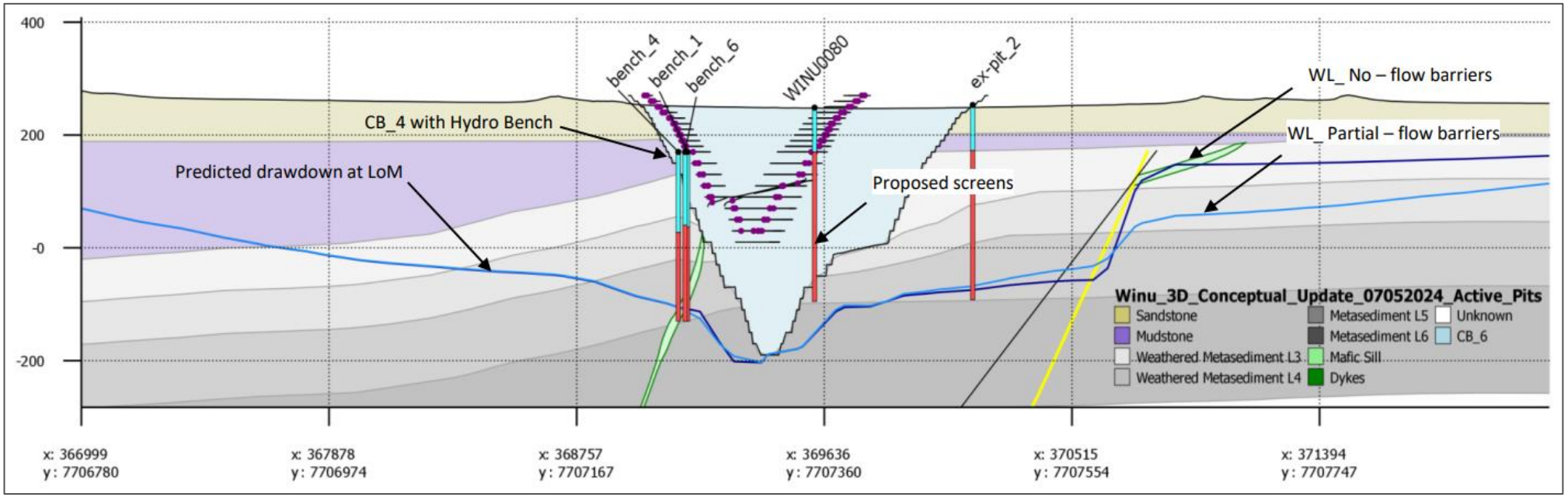

Source: Worley (2024b)

Notes: An excerpt from Figure 9-14 in the original document.

Figure 3.4: Conceptual drawing of seepage pathways toward the Winu pit

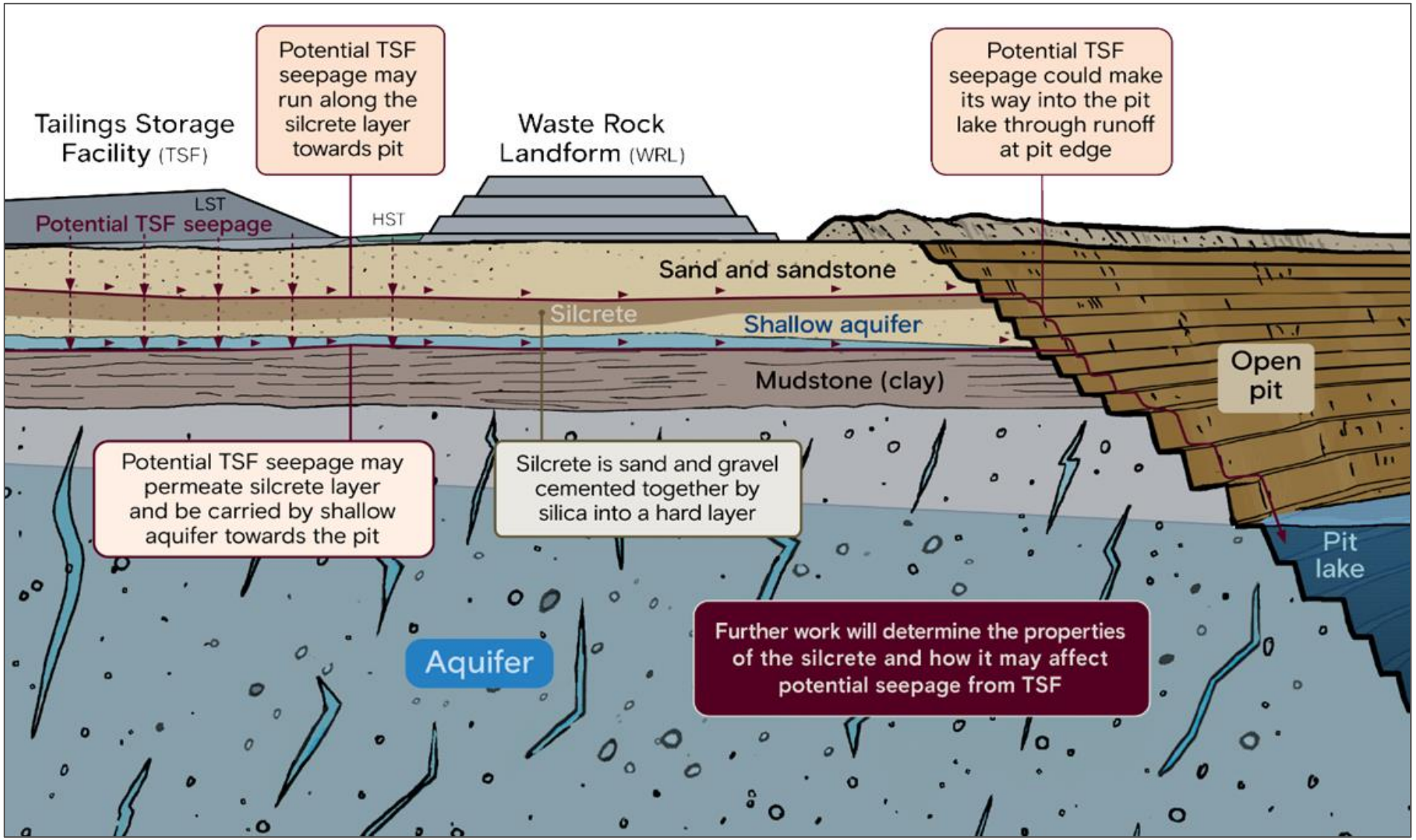

Source: Rio Tinto

Figure 3.5: Presence/absence map of silcrete in drill holes across TSF footprint

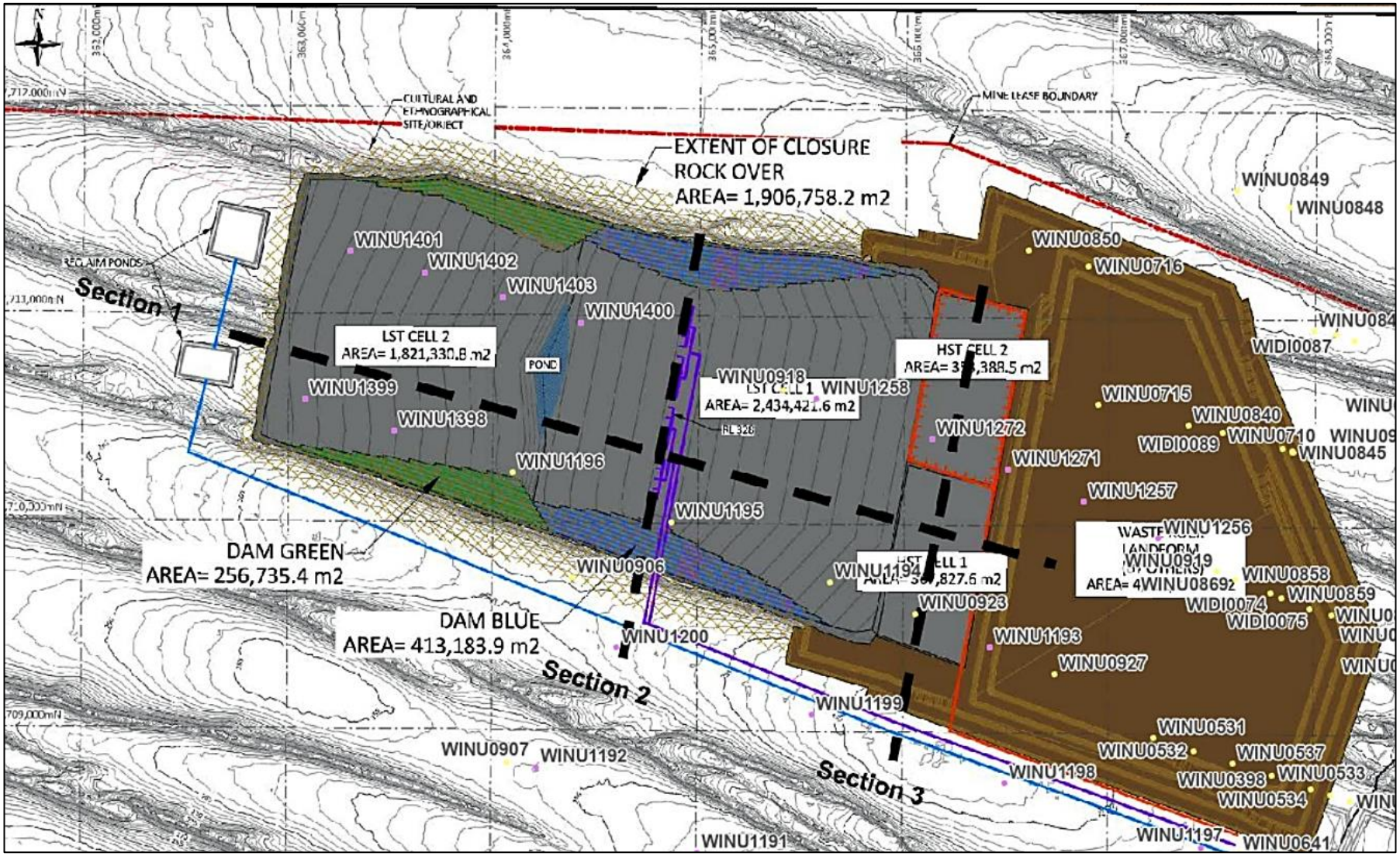

Source: Modified after WWL (2024b)

Notes: Drill holes shown as pink circles (•) contain logged silcrete intervals, whereas drill holes shown as yellow circles (•) do not feature silcrete.

3.2.3 Basal seepage rates

Seepage leaving the base of TSF cells would be expected to percolate downward. Modelling presented in O'Kane (2020) indicated that net seepage from the LST cells would range from <1% annual rainfall (constrained by the presence of a basal liner) to an upper bound of order 9% annual rainfall for LST cells with a thin metasediment cover (0.5–1 m plus 0.3 m topsoil) and no basal liner (i.e. free-draining). For the lower bound seepage flux, seepage residence times (per metre) may be decades (Figure 3.6).

Figure 3.6: Estimated water residence times in 1 m of unsaturated medium

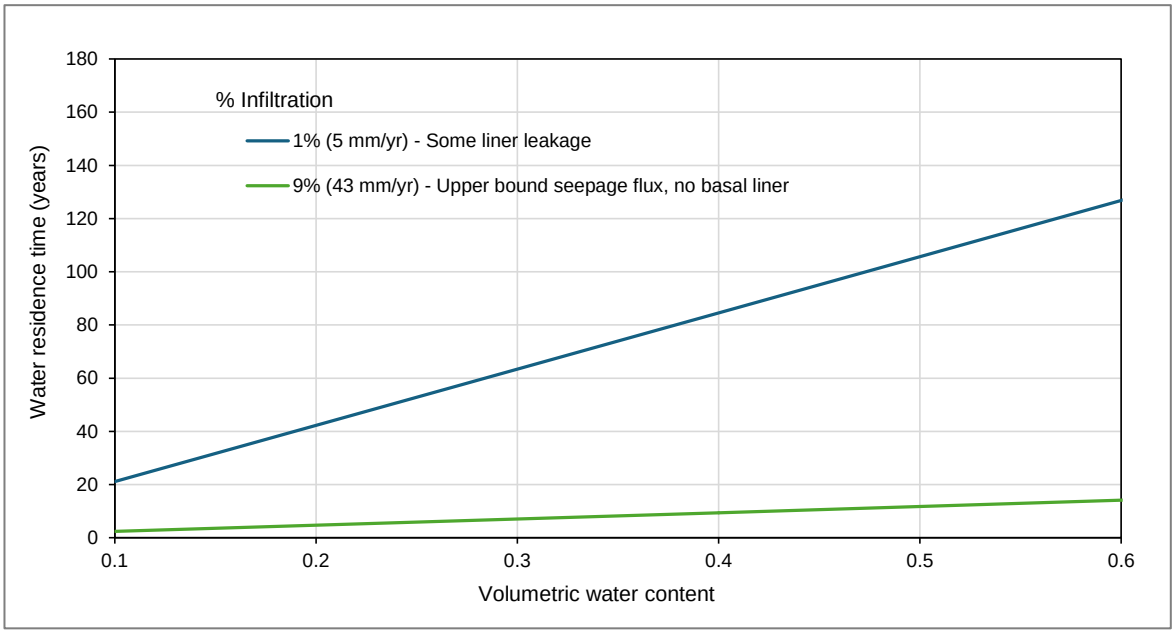

Source: RTS282_misc.xls

For the HST cells, modelling (O'Kane, 2024) suggested a similar range of basal seepage rates could apply, i.e. ranging from <1% annual rainfall to between 2% and 7% following possible degradation of the basal liner.

Beneath the TSF, the underlying strata comprise up 70 m of unsaturated material (Table 3.1, including all materials to the top of the Permian mudstone). This thickness of unsaturated material is reduced to 15 m if a perched aquifer is present above a low-permeability silcrete horizon (discussion in Section 3.2.2). The indicative vertical hydraulic conductivities presented in Table 3.1 are invariably higher than the estimated rates of seepage through the basal liner. Rates of seepage through the unsaturated zones will therefore be limited by the liner performance and/or net percolation rates rather than the properties of the underlying strata.

For a 70 m thick depth of unsaturated materials beneath the TSF (i.e. assuming the silcrete is absent), based on the seepage fluxes outlined above, seepage residence times within the unsaturated materials would be over a thousand years in the case of the lower bound (<1% rainfall) seepage estimates. For a reduced thickness of unsaturated material (15 m; i.e. assuming the silcrete is present and acts as an aquitard), the seepage timeframes would be reduced to centuries (e.g. 300 years for a volumetric water content of 0.1).

Table 3.1: Conceptual stratigraphic sequence beneath TSF

Unit	Hydraulic function	Indicative vertical hydraulic conductivity (mm/day)[1]	Silcrete present		Silcrete absent	
			Depth (m BGL)	Assumed depth to water table	Depth (m BGL)	Assumed depth to water table
Aeolian sands	Unsaturated aquifer	5,000 (100–1,000)	0–15	15	0–30	N/A
Silcrete	Aquitard	4	15–30		N/A	N/A
Sandstone	Partially saturated aquifer	100 (10–200)	30–80	N/A	30–80	70[2]
Permian mudstone	Aquitard	-	80+	N/A	80+	N/A

Notes:

[1] Ranges of vertical hydraulic conductivity from Advisian (2023).

[2] Saturated depth of the sandstone aquifer was estimated to vary between 5 m and 10 m (Golder, 2022).

3.2.4 Closure conditions and model case parameters

Rio Tinto's preferred cover designs, as adopted for this assessment, are:

- LST Cell 1 and 2: Tailings covered with 0.5–1 m metasediment waste rock and a shallow topsoil cover (0.3 m) at closure.
- HST Cell 1 and 2: Tailings covered with 6 m LST, overlain by 0.5 m metasediment waste rock at closure.

Key parameters used to describe the hydrological and physical conditions expected for the TSF post closure were aligned with those adopted for related tailings closure cover performance modelling (O'Kane, 2020, 2024) (Table 3.2).

Cover system performance was modelled based on projected, future climate conditions developed by O'Kane (2024) (SSP2-4.5). The SSP2-4.5 projection adopted by this and related studies predicts increased average temperatures (2–3°C) and decreased average rainfall (-4%) relative to the baseline (1991–2020).

For LST cells, the following model cases were assessed:

- Base case:

  A net percolation (NP) of <1% annual rainfall is predicted for the LST, given the expectation that basal seepage will be minimised by the BGM liner (O'Kane, 2020). Under this scenario, liner hydraulic conductivity would be $<1 \times 10^{-10}$ m/s, consistent with performance estimates of the LLDPE liner when >80% intact (O'Kane, 2024). An NP value of 1% (5 mm/year; 1.5×10^{-10} m/s) was adopted for the base case assessment.

- Sensitivity case:

  Estimated NP values considered by O'Kane (2020) are ≤9% annual rainfall, consistent with free-draining conditions where the BGM liner does not limit seepage or NP. An NP value of 9% (43 mm/year; 1.4×10^{-9} m/s) was adopted for the sensitivity case assessment.

For HST cells, the following cases were assessed:

- Base case:

  A NP of 1% annual rainfall is predicted for the HST cells, given the expectation that basal seepage will be minimised by the LLDPE liner (O'Kane, 2024). Under this scenario, liner hydraulic conductivity would be $<1 \times 10^{-10}$ m/s, consistent with performance estimates of the LLDPE liner when >80% intact (O'Kane, 2024).

- Sensitivity case:

  An NP of 6% annual rainfall is predicted for the HST cells when progressive degradation of the LLDPE liner is assumed (O'Kane, 2024).

Table 3.2: TSF closure scenario parameters

Type	Parameter	LST Cell 1	LST Cell 2	HST Cell 1	HST Cell 2
Facility physical parameters	Tailings footprint (m^2)[1]	2,434,422	1,821,331	367,828	358,389
	Max. bed depth (m)[2]	80	65	30	25
	Avg. settled dry density (t/m^3)[1]	1.55		1.36	
	Operations period (year)[3]	28			
Hydrological parameters	Avg. rainfall (mm/year)[4]	473 (SSP2-4.5)			
	Volumetric water content (dimensionless)[4]	0.45		0.56	
	Process water drain-down period at closure (year)[3]	10		N/A	
	Tailings saturation (%)[1]	>60%		>85%	
	Basal liner[1]	Bituminous geomembrane		■ 1.5 mm linear low-density polyethylene ■ Low permeability compacted soil	
	Lower bound basal liner hydraulic conductivity with degradation (m/second)[4]	■ LoM year 0–20: 10^{-12} ■ LoM year 20–35: 10^{-12} ■ LoM year 35–50: 10^{-11} ■ LoM year 50–100: 10^{-10} ■ LoM year 100–200: 10^{-9} ■ LoM year 200+: 10^{-8}			

Notes: 'LoM year' describes the life of mine year (0–28 operations; >28 post closure).

[1] WWL (2024b).
[2] WWL (2024c).
[3] WWL (2024d).
[4] O'Kane (2024).

4 Sulfide oxidation assessment

4.1 Theoretical considerations

Oxidation within the TSF is expected to be controlled by supply of oxygen (in air) from the surface. Due to the fine-grained nature of the tailings, it is expected that the supply of oxygen will be limited to diffusion. Illustrative examples of diffusion-controlled oxygen profiles are shown in Figure 4.1.

The first profile (a) shows the effect of oxygen diffusing into exposed tailings. The active oxidation zone is located immediately below the tailings surface. With time, as sulfides are depleted within the near-surface layer, oxygen would need to diffuse deeper into the tailings and oxidation would slow (due to the reduction in oxygen concentration gradient that drives diffusion). Concurrently, the rate of solute generation will slow.

The presence of a cover (as illustrated in Figure 4.1 (b)) will reduce the oxidation rates from the time that the cover is placed because the oxygen must diffuse through the cover before it enters the tailings. The effectiveness of the cover will depend on the effective oxygen diffusion coefficient of the cover materials – the lower the diffusion coefficient, the more effective the cover will be. For the same reason noted above, as the oxidation zone progresses into the tailings, oxidation rates will slow over time.

As noted in Section 2.3.4, the main purpose of the proposed cover design for the HST is to decouple the tailings from the evapotranspiration zone thus reducing upward water loss from underlying HST. The thickness of the proposed cover (>6 m) would also be expected to have some benefits in slowing oxygen diffusion to the HST. The primary purpose of the cover on the LST is to limit erosion from high-intensity rainfall events and minimise dust emissions, including vegetation establishment. The cover is thin (up to 1 m with topsoil) and is expected have a negligible influence on oxygen ingress.

Oxygen diffusion coefficients are strongly influenced by the degree of saturation in the pore space (i.e. moisture content). As discussed already (Section 2.3.4), saturation in the HST cells is expected to remain high, and therefore diffusion is expected to be very slow. In the LST cells, over time, the tailings are expected to desaturate and rates of oxygen diffusion would be higher.

Figure 4.1: Illustrative oxygen diffusion profiles as a function of depth below the surface of the tailings

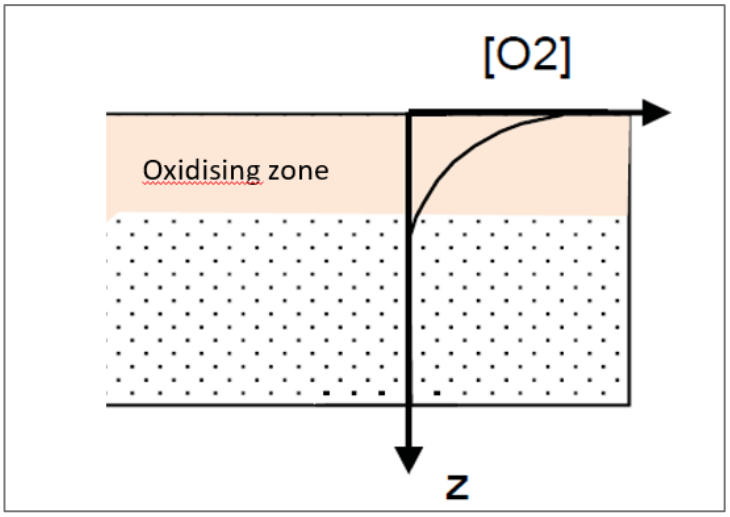

(a) Oxidation in near-surface layer – oxygen supply by diffusion

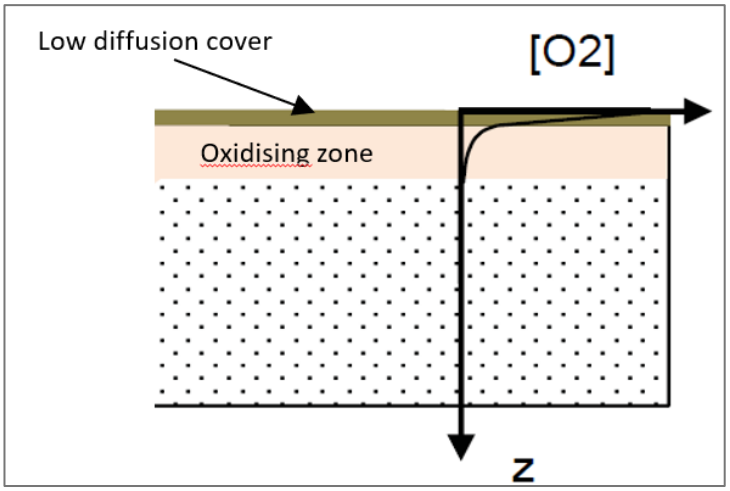

(b) Oxidation in tailings beneath a low diffusion coefficient cover layer

Source: Modified from Garvie et al. (2014)

The key rate-determining factors for sulfide oxidation in the tailings will be:

- Intrinsic oxidation rate – the rate at which sulfide minerals such as pyrite oxidise where oxygen supply is not limited (i.e. by moisture saturation).
- Bulk oxygen diffusion coefficient – describes the rate at which oxygen diffuses through porous media. Diffusion coefficients are a function of degree of saturation, as well as particle size distribution.
- Oxygen diffusion path length – the thickness of material through which oxygen must diffuse prior to reaching un-oxidised sulfide minerals. The presence of covers and the depth of oxidised tailings will contribute to the path length.

The derivation of these key parameters is discussed further in the following sections.

4.2 Laboratory-scale sulfide oxidation rates

Intrinsic oxidation rates (IORs) were determined from kinetic leach column (AMIRA and humidity cell tests) sulfate leachate results (Rio Tinto, 2024b). The IOR calculations assumed that the sulfur was present as pyrite, sulfide is oxidised to sulfate, and that all the sulfate is fully leached from the sample. The calculation is based on stoichiometry for the oxidation of pyrite as follows:

$$FeS_2 \text{ [pyrite]} + 3.75\ O_2 + 3.5\ H_2O \Leftrightarrow 2\ SO_4^{2-} + 4\ H^+ + Fe(OH)_3 \text{ [ferric hydroxide]} \quad (1)$$

Oxygen consumption rates (OCRs), determined from oxygen concentration depletion in a sealed atmosphere (SRK, 2020), were also available for two tailings samples.

The oxidation rate adopted for LST (4.4×10^{-11} kg O_2 kg^{-1} s^{-1}) was based on the mean oxidation rate obtained from results for six LST samples with sulfur concentrations ranging from 0.18 wt%S to 0.4 wt%S. The dataset comprised five kinetic columns (IORs) and one OCR measurement.

Given there are currently no kinetic data for samples representing HST due to the lack of mass generated during metallurgical study test programs, it was necessary to extrapolate an appropriate oxidation rate from multiple lines of evidence:

- Linear extrapolation using oxidation rates for LST samples, based on the relationship with sulfide sulfur concentration. The extrapolated rate was in the order of 3×10^{-9} kg O_2 kg^{-1} s^{-1}.
- Corroboration with oxidation rates obtained for highly sulfidic tailings (22 wt%S) assessed as part of previous SRK projects. The determined average oxidation rate (1.9×10^{-9} kg O_2 kg^{-1} s^{-1}) was consistent (i.e. same order of magnitude) with the extrapolated rate.

Based on these lines of evidence, an oxidation rate of 3×10^{-9} kg O_2 kg^{-1} s^{-1} was adopted for the HST.

4.3 Bulk oxygen diffusion coefficients

Bulk oxygen diffusion coefficients (D_o) for LST and HST were selected from published values. A range of values from the scientific literature were compiled, where tailings media were of similar texture and moisture content (Table 4.1). The LST texture is described sandy silt and seepage rate modelling (WWL, 2024c) predicted that LST saturation will be maintained in order of at least 50% (50–80%). The HST texture is described as silty clay, with long-term saturation predicted to be >85% (O'Kane, 2024).

Values adopted for this assessment, as informed by published values, were 7×10^{-7} m^2 s^{-1} for LST and 3×10^{-9} m^2 s^{-1} for HST (base case). The low value adopted for the HST is analogous to that applicable for diffusion through water.

Table 4.1: Relevant literature values for oxygen diffusion coefficient

Tailings type	Texture	Moisture	Oxygen diffusion coefficient ($m^2 s^{-1}$)	Source
LST	Silty loam	'Wet'	1.5×10^{-8}	Alakangas et al. (2008)
	Silt loam	60% saturation	3.2×10^{-7}	Vincent et al. (2006)
	Silt loam	60% saturation	3×10^{-7}	Demers et al. (2009)
		50% saturation	7×10^{-7}	
HST	Silty clay loam	'Wet'	1.9×10^{-8}	Alakangas et al. (2008)
	Silty	90% saturation	2.9×10^{-9}	

4.4 Calculation of field-scale sulfide oxidation rates

A constant intrinsic oxidation rate model was used to predict rates of sulfide oxidation, based on the approaches described in Ritchie (1995) and Garvie et al. (2014).

Some key features/considerations of the model approach used:

- Intrinsic rate of sulfide oxidation remains constant over time.
- Oxygen transport, and therefore sulfide oxidation, is diffusion-controlled and advective gas transport is not considered.
- Model considers average sulfide sulfur content, represented as pyrite. While the tailings may also contain pyrrhotite, pyrrhotite oxidation stoichiometry is less predictable than pyrite. Therefore, all sulfide was assumed to be present as pyrite.
- Tailings are modelled as homogeneous with respect to particle size distribution and moisture saturation (i.e. oxygen diffusion), sulfide mineral distribution and physical parameters such as bed thickness over the facility footprint.

In the case of the LST cells, the proposed metasediment waste rock cover (0.5–1 m plus 0.3 m topsoil) was considered to have a negligible influence on diffusion-limited oxygen supply through the tailings bed and was not represented in the model.

For the HST cells, the oxidation modelling accounted for a 6 m thick cover of LST. The model predicted that the 6 m LST cover would be fully oxidised within 20 years of placement, with comparatively minimal influence on the long-term rate of solute generation and seepage composition within the underlying HST. The LST cover was therefore represented in the HST oxidation model as a geochemically inert layer.

Key input parameters used for oxidation modelling are given in Table 4.2.

Table 4.2: Key oxidation model input parameters

Model parameter	LST Cell 1	HST Cell 1
Maximum tailings bed thickness (m)[1]	80	30
Avg. dry density (t/m^3)[2]	1.55	1.36
Sulfide-S (wt%S)[3]	0.2	21.5
Cover[4]	None	6 m LST
Average saturation (%)\[4]	60	85
Bulk oxygen diffusion coefficient (m^2 s^{-1})	7×10^{-7}	3×10^{-9}
IOR (kg(O_2)/kg(tailings)/s)	4.4×10^{-11}	3.0×10^{-9}
IOR (kg(O_2)/m^3(tailings)/s)	6.82×10^{-8}	4.08×10^{-6}

Notes:

[1] WWL (2024c).
[2] WWL (2024b).
[3] Rio Tinto (2024b).
[4] O'Kane (2024).

4.5 Results

The LST is predicted to oxidise over multi-century timescales with LST Cell 1, the deepest of two proposed LST cell beds, predicted to be fully oxidised to 80 m after around 3,000 years. This is due to relatively low reactivity (IOR), the time required to consume sulfides present, and the expectation that oxygen diffusivity remains low post closure. Note that the oxidation rate declines substantially during the initial 50 years projected, as the oxidation front progresses to greater depths (Figure 4.2). After 300 years, the oxidation front is predicted to develop to 25 m below the LST surface.

Oxidation of HST is predicted to be very slow, whereby only the topmost 0.1–0.2 m is predicted to have oxidised after 300 years (Figure 4.3). This is due to the high degree of saturation to be maintained for the HST cells post closure, limiting the supply of oxygen, combined with the high abundance of sulfide (>20 wt% sulfide sulfur) in the HST. The calculated landform oxidation rate decreases rapidly during the initial 100 years. Under base case and sensitivity case conditions, the phreatic surface within the HST is expected to be about 1.5 m below the HST surface. The oxidation front is not expected to proceed beyond the phreatic surface. For context, the time required to oxidise the top 1 m of HST would be in the order of 10,000 years.

Figure 4.2: Predicted oxidation rate of LST (Cell 1)

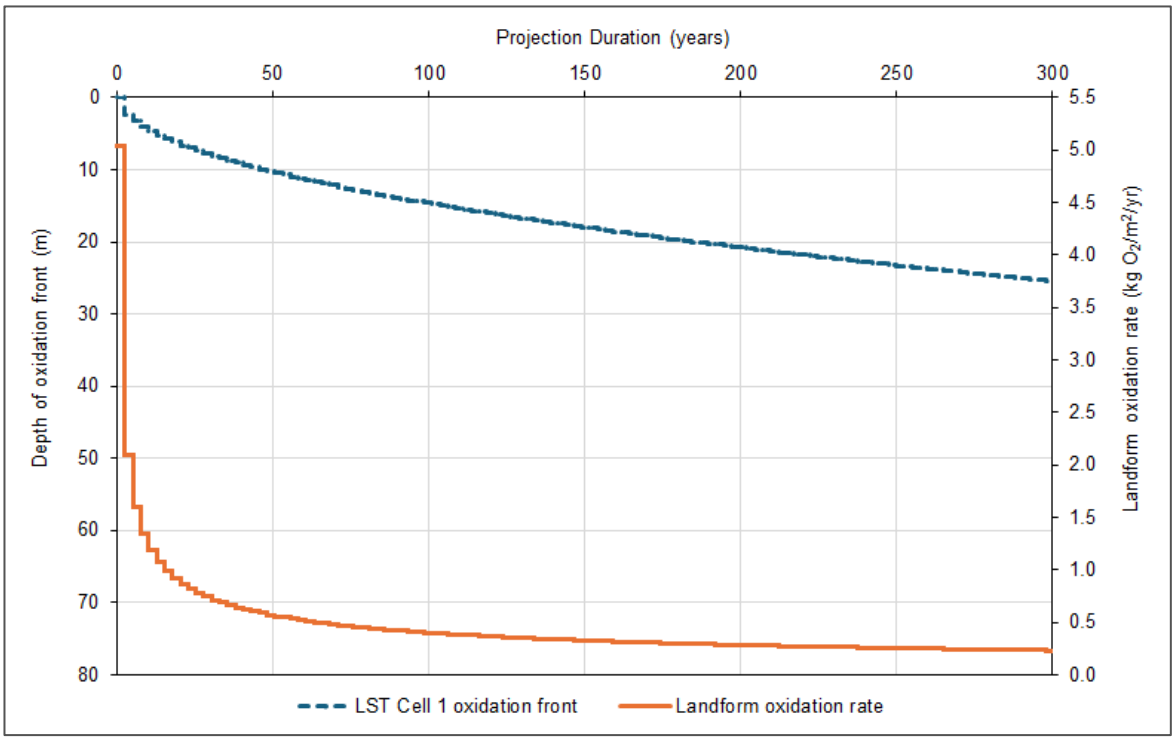

Figure 4.3: Predicted oxidation rate of HST (Cell 1)

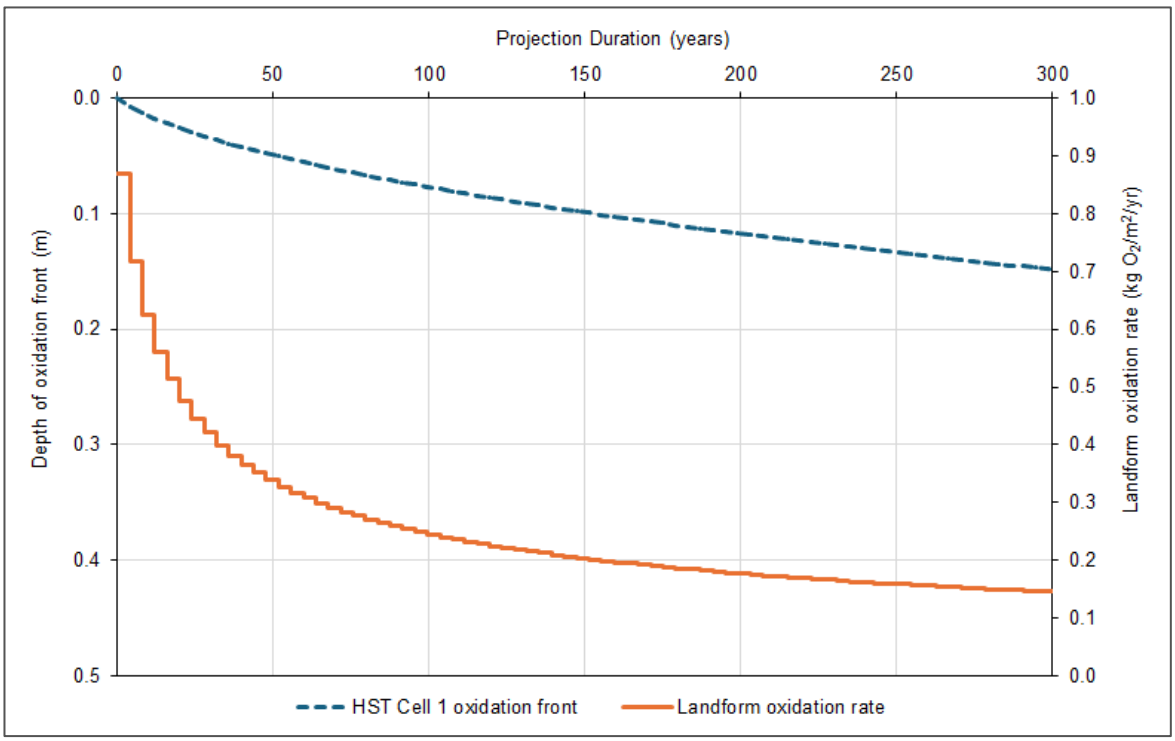

5 Calculated post-closure TSF seepage quality

5.1 Low sulfur tailings

5.1.1 General approach

Calculations focused on estimating the mass of solute produced within a representative column (area 1 m^2) of tailings. Sulfate production rates (Section 4) were combined with element-to-sulfate mass ratios (Section 5.1.3) to calculate the mass of leachable solute generated within the column over a given period. The resultant leachable mass was dissolved, conceptually, in the relevant porewater flux volume for a given period of time. Porewater flux was estimated from net percolation (as limited by the TSF cover, if present) to generate total solute concentrations in seepage that reaches the base of the TSF cells.

Using the geochemical speciation modelling code, PHREEQC (Parkhurst et al., 2013), the calculated solute concentrations were adjusted to account for potential mineral and gas interactions and yield a corresponding dissolved solute concentration estimate. To represent acid neutralisation capacity in the LST, the PHREEQC simulations included calcite in the equilibrium mineral assemblage.

It should be noted that some cases resulted in high solute concentrations outside the confidence limits of the thermodynamic data (minteq V4) for the model; in these cases, uncertainty exists as to the estimated equilibrium controls.

It should be acknowledged that short-medium term post-closure seepage quality is expected to be dominated by residual process water[2]. Due to the slow percolation rates within the tailings (Section 5.1.1), basal seepage is unlikely to reflect sulfide oxidation products generated near the tailings surface until many centuries have elapsed.

5.1.2 Sulfate profiles

Figure 5.1 presents illustrative long-term projections of solute concentration trends in LST Cell 1 represented by sulfate. The sulfate release profiles show the following attributes:

- Gradual increasing concentration at early times as the first pore volume is displaced.
- Plateaus occur while concentrations are approximately constant, being controlled by the relationship between sulfate production rate (or solubility limits, which are not represented in the profiles illustrated in Figure 5.1) and elution rate. There may be multiple plateaus reflecting changes to conditions in the tailings column.
- Concentration decreases due to the depletion of reactive sulfides and leaching of soluble weathering products from the LST profile.

[2] The LST process water is indicated to be slightly basic (pH 8) with alkalinity in the order of 100 mg/L as $CaCO_3$. Relative to groundwater in the underlying shallow aquifers (Section 2.2), process water (Section 2.3.2) is indicated to have higher concentrations of sulfate and a range of metals/metalloids (Cd, Co, Cu, Mo, Ni, Pb, Sb, Se, Tl, U) inferred to be associated with partial oxidation of sulfides during ore processing.

Figure 5.1: Projected long-term LST seepage quality trends

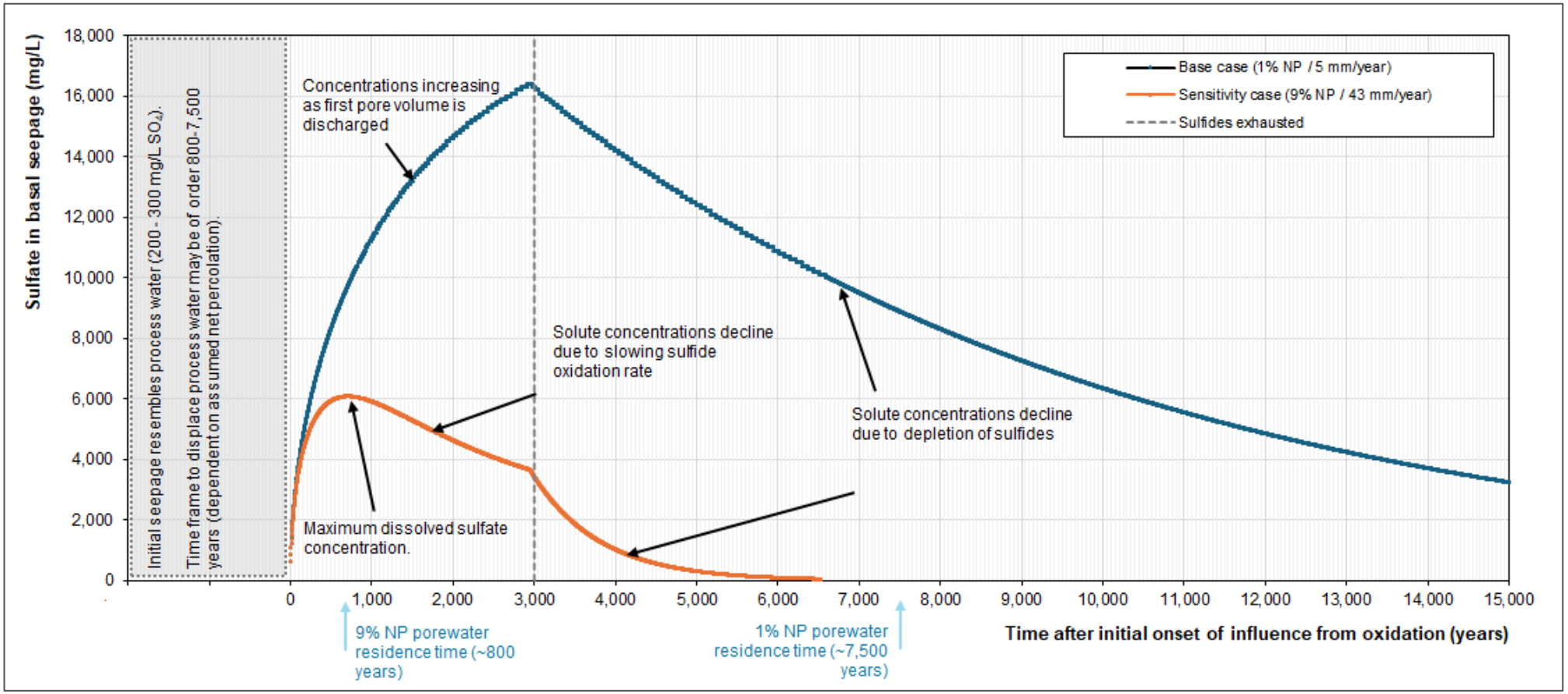

Source: RTS282 Winu Seepage Model Collated Cases.xlsx

Notes: Sulfate concentrations shown do not reflect the influence of geochemical processes such as secondary mineral precipitation.

For the sulfate profiles estimated in the current study, net percolation rates and corresponding tailings porewater residence time significantly influence the evolution. For very low net percolation rates (i.e. 1% annual rainfall), relatively high concentrations develop due to a low rate of flushing by meteoric water. With higher net percolation (i.e. 9% annual rainfall), solutes are dissolved in a larger volume of percolate, leading to lower concentrations and more rapid flushing of oxidation products.

In the base case (1% net percolation), porewater residence time is estimated to be in the order of 7,500 years, which is longer than the time for complete oxidation of sulfides present (~3,000 years). Increasing sulfate concentrations are therefore 'cut off' before completion of a pore volume exchange. Following depletion of the sulfides, sulfate and other oxidation products would be flushed from the tailings and seepage concentrations would decline accordingly.

Porewater residence time for the sensitivity case (9% net percolation) is estimated at 800 years. Sulfate concentrations in seepage are calculated to increase during this time. As sulfide oxidation is predicted to be ongoing at ~800 years post closure, an approximate plateau occurs – initially higher, reflecting the earlier higher oxidation rates while the oxidation zone is close the surface, and then declining as the oxidation rate decreases. Following depletion of sulfides, a typical flushing profile is shown. Note that calculations have not taken into account processes such as dispersion along transport pathways. The calculations are therefore considered conservative as the peak concentrations may have been overestimated.

5.1.3 Solute production

Elemental sulfate mass ratios representative of production ratios during oxidation have been informed by data obtained in kinetic (column) test programs. At near-neutral pH, column leachate composition is unlikely to reflect rates of metal/metalloid production linked to sulfide oxidation for solubility constrained parameters, including secondary mineral solubility and adsorption controls. To account for this, reference was made to columns generating acidic leachate despite some of these columns containing material not directly representative of the LST in terms of average sulfide-S content. These columns are less likely to be influenced by secondary mineral solubility and adsorption controls. To reflect the near-neutral conditions expected in the bulk LST under field conditions (Section 3.2.1), carbonate-based neutralisation was represented in geochemical models (PHREEQC) by reaction with calcite when calculating seepage composition. Selected properties of the nominated samples are given in Table 5.1.

The resulting element-to-sulfate mass ratios are provided in Table 5.2. Only solutes noted to be present above detection limits in the kinetic tests were included in the source term for tailings oxidation. The elements incorporated in the source terms included:

- metals/metalloids known or inferred to be present in the sulfide minerals present (pyrite, pyrrhotite, chalcopyrite) during oxidative dissolution
- elements inferred to be released as an indirect consequence of sulfide oxidation (e.g. carbonate or silicate dissolution in response to acidity generated)
- metals/metalloids with changed solubility resulting from variations in pH.

Table 5.1: Summary of kinetic column samples used to inform solute production rates

Parameter	Unit	LS tailings – High sulfur (PS feed)	LS tailings – High sulfur (SS feed)
Method	-	Humidity cell	Humidity cell
Tailings sample stratigraphy	-	Primary sulfides	Secondary sulfides
Test duration	-	91 weeks	91 weeks
Stable period	-	Weeks 50–91	Weeks 50–91
Stable leachate pH	SI	5.17	3.36
Total sulfur	wt%S	0.55	0.36
Oxidised sulfur	wt%S	0.03	0.06
Sulfide sulfur	wt%S	0.52	0.3
AP	kg H_2SO_4/t	16	9.2
ANC	kg H_2SO_4/t	15	7
NPR	-	0.89	0.64
NAG pH	SI	5.2	5.0
NAG (pH 4.5)	kg H_2SO_4/t	<0.1	<0.1
NAG (pH 7)	kg H_2SO_4/t	1.5	1.5
NAPP	kg H_2SO_4/t	2	4
Class (AMIRA)	-	UC	UC
Class (MEND)	-	PAF	PAF

Source: Rio Tinto (2020b)

Notes: PS – primary sulfides; SS – secondary sulfides; AP – acid potential; UC – uncertain.

Table 5.2: Element-to-sulfate mass ratios for estimation of tailings seepage solute composition

Parameter	LST
Calcium	9×10^{-2}
Magnesium	1.3×10^{-1}
Sodium	2.3×10^{-2}
Potassium	3.7×10^{-2}
Chloride	5.4×10^{-3}
Fluoride	8.8×10^{-5}
Aluminium	7.5×10^{-4}
Antimony	-
Arsenic	-
Barium	3.3×10^{-5}
Beryllium	2.3×10^{-5}
Boron	-
Cadmium	2.3×10^{-5}
Chromium	2.9×10^{-4}

Parameter	LST
Cobalt	2.6×10^{-3}
Copper	4.9×10^{-3}
Iron	5.7×10^{-2}
Lead	3.8×10^{-4}
Lithium	2.1×10^{-4}
Manganese	4×10^{-3}
Molybdenum	-
Nickel	2.6×10^{-3}
Selenium	-
Silicon	8.7×10^{-2}
Silver	-
Strontium	1.7×10^{-4}
Thallium	-
Tin	-
Uranium	1×10^{-4}
Vanadium	-
Zinc[1]	5×10^{-3}

Notes: Hyphens (-) denote where an element was <LOD and therefore inferred to be absent from solution.

[1] The sulfate mass ratio for zinc, based on KCl or synthetic acid and metalliferous drainage data, resulted in unrealistically high elution to seepage based on mass balance calculations. The ratio was therefore based on NAG liquor data.

5.1.4 Results

To gain insight to the potential composition of long-term seepage (influenced primarily by sulfide oxidation processes), calculated seepage composition (Table 5.3) for base and sensitivity case conditions indicate the following:

- Circumneutral conditions are maintained (pH 7–8) in the base case and sensitivity cases, with net alkalinity in the order of 200–300 mg/L as $CaCO_3$. An acidic sensitivity case is also presented, to evaluate a case where ANC was insufficient to maintain pH neutral conditions. For this sensitivity case, carbonate-based neutralisation was not represented in geochemical models (PHREEQC) when calculating seepage composition.
- Sulfate is the dominant solute, typically comprising >70% of the total dissolved solids (TDS). Maximum predicted sulfate concentrations are higher under base case conditions (12,000 mg/L) compared with the sensitivity case (5,300 mg/L). Note that where solubility controls exert only minor influence, concentrations are expected to be lower under sensitivity case conditions due to increased dilution by meteoric water.
- Concentrations of aluminium, barium, calcium, copper, iron, lead, magnesium, manganese, potassium, silicon and zinc are also predicted to be constrained by secondary mineral precipitation within the tailings bed (Table 5.4). Solution pH can exert a strong control on solubility; for example, dissolved concentrations of elements such as Cu and Fe are calculated to be significantly higher in acidic sensitivity case.

Table 5.3: Estimated LST cell basal seepage composition at long-term peak solute concentrations

Parameter	Unit	Base case (2,600 years[1])	Sensitivity case (800 years[1])	Acidic sensitivity case (800 years[1])	Reference
		1% net percolation (5 mm/year) Liner intact	9% net percolation (43 mm/year) Liner degraded	1% net percolation (insufficient ANC)	Sandstone aquifer
pH	s.u	7.5	7.4	4.1	7.4
Total alkalinity	mg/L as $CaCO_3$	320	220	-	110
Acidity	mg/L as $CaCO_3$	-	-	52	-
Ca	mg/L	390	470	380	17
Mg	mg/L	2,200	800	2,100	8
Na	mg/L	380	140	380	120
K	mg/L	600	220	600	8
SO_4	mg/L	12,000	5,300	14,000	28
Cl	mg/L	88	33	88	120
F	mg/L	1.4	0.54	1.4	0.5
Ag	mg/L	0.00018	0.00013	2	0.00001
Al	mg/L	0.0002	0.0002	0.0002	0.03
As	mg/L	0.003	0.003	0.003	0.003
B	mg/L	0.0024	0.0035	0.0022	0.24
Ba	mg/L	0.38	0.14	0.38	0.16
Be	mg/L	0.24	0.24	0.24	0.0001
Cd	mg/L	0.38	0.14	0.38	0.0001
Co	mg/L	4.7	1.8	4.7	0.0001
Cr	mg/L	42	16	42	0.001
Cu	mg/L	0.63	0.65	80	0.004
Fe	mg/L	0.00013	0.00015	800	0.2
Li	mg/L	0.22	0.18	5	0.0051
Mn	mg/L	3.4	1.3	3.4	0.11
Mo	mg/L	7.5	6.8	66	0.0055
Ni	mg/L	0.0055	0.0055	0.0055	0.002
Pb	mg/L	42	16	42	0.0003
Sb	mg/L	0.00025	0.00025	0.00025	0.0002
Se	mg/L	7.5	7.7	7.3	0.00025
Si	mg/L	0.00001	0.00001	0.00001	28
Sn	mg/L	2.8	1	2.8	0.0003
Sr	mg/L	0.00002	0.00002	0.00002	0.29
Tl	mg/L	0.0003	0.0003	0.0003	0.00002
U	mg/L	1.6	0.62	1.6	0.00018
V	mg/L	0.0012	0.0012	0.0012	0.0012
Zn	mg/L	39	29	82	0.009

Notes:

[1] Peak seepage concentrations would occur only after long time periods had elapsed, about 2,600 years for the low infiltration cases (1% NP), and around 800 years for the higher infiltration case (9% NP).

[2] The modelled conditions within the tailings were elevated partial pressure of CO_2 (0.3v/v%) and pe was set to comply with the relationship pe + pH =14 (i.e. relatively oxic). The median groundwater composition for the sandstone aquifer is shown for comparison with seepage.

Table 5.4: Solubility controls affecting tailings seepage

Mineral phase	Formula	Solutes affected	Base case	Sensitivity case	Alternative sensitivity case
Alunite	$KAl_3(SO_4)_2(OH)_6$	Al, K, SO_4			✓
Anglesite	$PbSO_4$	Pb, SO_4			✓
Barite	$BaSO_4$	Ba, SO_4	✓	✓	✓
Calcite	$CaCO_3$	Ca	✓	✓	
Cerussite	$PbCO_3$	Pb	✓	✓	
Chalcedony	SiO_2	Si	✓	✓	✓
Diaspore	α-AlO(OH)	Al	✓	✓	
Ferrihydrite	$(Fe^{3+})_2O_3 \cdot 0.5H_2O$	Fe	✓	✓	✓
Gypsum	$CaSO_4 \cdot 2H_2O$	Ca, SO_4	✓	✓	✓
Langite	$Cu_4(SO_4)(OH)_6 \cdot 2H_2O$	Cu, SO_4	✓	✓	
Rhodochrosite	$MnCO_3$	Mn	✓	✓	
Smithsonite	$ZnCO_3$	Zn	✓	✓	

Notes: Tick marks indicate which mineral phases were saturated (predicted to precipitate) under each model case. Secondary mineral phases allowed to precipitate in speciation models were those judged to be plausible under the given geochemical conditions with reference to Nordstrom and Alpers (1999).

5.2 High sulfur tailings

Trends in seepage solute concentration over time are consistent with those presented for LST (Section 5.1.1) in terms of potential sulfate concentration maxima. Long-term, illustrative projections indicate that seepage concentrations would increase over the course of thousands of years under base case conditions and over hundreds of years under sensitivity case conditions, before declining over protected timeframes.

The similarities between predicted seepage evolution trends for LST and HST can be attributed to HST storage conditions. Although the HST have greater potential to generate acidity, storage under highly saturated conditions is predicted to limit sulfide oxidation to thin layers at the tailings bed surface. Given Rio Tinto's expectation that most of the HST volume will remain saturated, only a minor proportion of the sulfide content may oxidise (≤5% assuming oxidation would not proceed beyond 1.5 m from the surface).

5.2.1 Medium term seepage quality

Calculated porewater residence times for HST are in the order of 3,500 years and 600 years under base case and sensitivity case conditions, respectively. As noted for LST, corresponding low rates of percolation indicate that seepage would resemble process water in the medium term (order of 300 years post closure).

The indicative HST process water composition is circumneutral (pH 7–8) and generally consistent with LST process water (Section 2.3.2). Relative to groundwater in shallow aquifers, HST process water contains elevated concentrations of sulfate and metals/metalloids (Cd, Co, Cu, Mn, Mo, Ni, Pb, Sb, Se, and Tl), inferred to reflect limited sulfide oxidation during processing trials.

5.2.2 Longer term seepage quality

For the first 300 years, the average rate of acid generation in HST Cell 1 is estimated to be 1×10^5 kg H_2SO_4/year.

The total ANC of the tailings bed (HST Cell 1) is estimated at 9×10^7 kg as H_2SO_4 in solids. The porewater alkalinity present is 2.8×10^5 kg as H_2SO_4 (0.3% of the ANC of solids).

At average rates of acid production, cumulative acidity produced would equal the ANC associated with porewater alkalinity within 3 years, and would equal the total ANC of the tailings bed solids in the order of 1,000 years, when the oxidation front is projected to progress to ~30 cm in depth. Based on these inferences and calculations, acidic conditions would not develop in HST cells until a prolonged period has elapsed.

In the very long-term (order of thousands of years), the oxidation front could progress beyond 30 cm, and net acidic conditions in porewater, and eventually in basal seepage, cannot be precluded. Note that, given the prolonged estimated porewater residence times (600–3,500 years), time required to transport acidity from near-surface tailings downwards may be very long. Basal seepage reflecting sulfide oxidation products may therefore remain non-acidic for at least 1,000 years.

Further progression of the oxidation front is more likely should the basal liner degrade, as reflected in the sensitivity case. Overall, there is a high level of uncertainty around potential for net acid conditions given the extremely long timeframes involved.

6 Groundwater impact assessment

This section provides an assessment of potential impacts of tailings seepage impact on groundwater and Winu pit lake quality.

Given the long timeframes involved with respect to the geochemical evolution of the TSF system, the following should be acknowledged:

- Slow basal seepage rates, and the presence of a significant thickness[3] of unsaturated material between the base of TSF and the groundwater table, suggest that the timeframes before groundwater could be impacted by TSF seepage are long – centuries to millennia.
- Initial phases of seepage will resemble process water. Process water is expected to be near-neutral with indicative composition as presented in Table 2.5. The duration of the initial phase could be expected to reflect the duration of 1–2 pore volume exchanges through the tailings cells (i.e. order of 800–7,500 years for the LST, and 600–3,500 years for the HST).
- Secondary phases of seepage would be more strongly influenced by oxidation of sulfides present in unsaturated tailings. For most reasonable assumptions, the secondary phases of seepage would not occur within the timeframes represented by the pit lake modelling (up to 300 years post closure).

6.1 Groundwater flow regime beneath the TSF

Some uncertainty remains around the hydrogeological conditions at Winu, particularly around terms of elevation differences (head) between for potential perched water tables and where water might seep on pit walls (i.e. ‘daylight’). Outputs from current hydrogeological investigations indicate very shallow gradients for perched water tables associated with silcrete and sandstone horizons. To enable estimates of potential groundwater flux, a head of 10 m was adopted between the water table beneath the TSF and where groundwater may potentially seep from the pit walls. This value reflects the estimated variability in the saturated thickness of the sandstone aquifer (5–10 m) (Golder, 2022) and requires further evaluation as more data become available for superficial aquifers.

Estimates of groundwater flux beneath the TSF (Darcy flux) were generated, assuming flow through a cross sectional area defined by the width of the TSF (1.6 km) and assumed depth of saturated zones within the aeolian sands (5 m) and sandstone aquifer (10 m), respectively. The estimates are presented in Table 6.1, along with estimates of TSF seepage flux for comparison.

[3] 15 m if silcrete present, 70 m where no silcrete present (Table 2.2).

Table 6.1: Estimates of groundwater flux beneath the TSF

Parameter	Minimum	Maximum	Comment
Groundwater flux (aeolian sands), m^3/year	12,000	51,000	Cross sectional area, 8,000 m^2 (see main text) and hydraulic conductivities, 2.2–5 m/day (WWL, 2024b; Advisian, 2023)
Groundwater flux (sandstone), m^3/year	1,000	6,600	Cross-sectional area, 8,000 m^2 (see main text) and hydraulic conductivities, 0.2–0.65 m/day (WWL, 2024b; Advisian, 2023)
Estimates of TSF seepage flux, for comparison			
LST	22,900 (base case; 1% infiltration)) 210,000 (sensitivity; 9% infiltration)		Assumed LST footprint, 485 ha
HST	400 (0.1% infiltration) 4,000 (base case; 1% infiltration)		Assumed HST footprint, 85.5 ha

Notes: Range of hydraulic gradients applied (0.002–0.004).

The groundwater fluxes are slow. The distance from the TSF to the pit ranges from 3 km to 6 km depending on position within the TSF footprint. Estimated groundwater travel times from the TSF footprint to the pit are in the order of 1,000–13,000 years for flow within the sandstone aquifer. In the less likely situation where groundwater travels through aeolian sand, travel times may be in the order of 150–1,300 years.

By any estimate, any groundwater potentially affected by TSF seepage would travel very slowly and would be unlikely to reach the pit until a substantial period had elapsed after operations cease. The slow movement of water through superficial aquifers is corroborated by dewatering studies indicating that pit inflows from the sandstone aquifer are expected to be minimal. This is due to expected low permeability of the underlying mudstone unit, limited saturated thickness of the sandstone unit and the absence of observed groundwater level responses in the sandstone units to high-intensity rainfall associated with Cyclone Blake in January 2020 (Golder 2022; Worley, 2024b).

6.2 Mixing of TSF seepage and groundwater

Noting that TSF seepage may take a long time to reach the groundwater table (Section 3.2.3), the potential mixing ratios that could apply have been estimated from the fluxes presented in Table 6.1. The range of mixing proportions are shown in Figure 6.1, and suggest that dilution of seepage by groundwater may be minor. Under base case conditions, proportions of seepage in the partially saturated sandstone aquifer range between 0.75 and 0.95 for LST (i.e. up to 25% dilution) and between 0.4 and 0.8 for HST.

Figure 6.1: Estimated proportion of TSF seepage in a mixing zone beneath TSF footprint

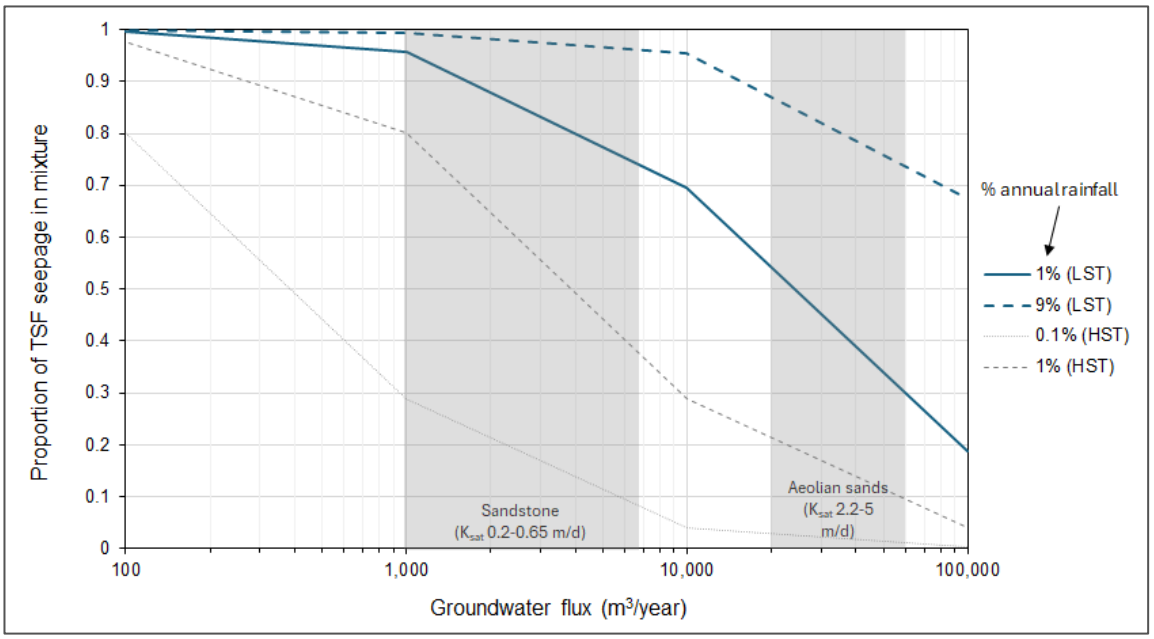

Notes: Prepared using flux estimates presented in Table 6.1.

In addition to dilution by groundwater along seepage pathways, it is expected some solutes may be attenuated due to water–rock interactions. Should secondary mineral precipitation occur at the point of mixing, some solute mass may be attenuated.

A series of calculations and geochemical modelling (PHREEQC) examined the mixing of LST seepage and groundwater were undertaken using a range of redox conditions (~60–400 mV) and CO_2 partial pressures (atmospheric – 0.03%v/v to highly elevated – 4%v/v[4]). Groundwater chemistry was based on the median values for the sandstone aquifer (Table 2.3, Section 2.2) and seepage chemistry was represented by the maximum estimated basal seepage concentrations (Section 5.1.4).

Figure 6.2 shows the results graphically for selected parameters assuming low and high bound redox and CO_2 partial pressure conditions. The calculated composition of mixtures, for intermediate geochemical conditions, are presented in Table 6.2 and Table 6.3.

Key findings from the simulation of seepage and groundwater mixing were:

- Modelled groundwater pH mostly varies between 6.5 and 8.0 depending on the redox and CO_2 equilibration conditions applied. Similarly, alkalinity varies between 120 and 650 mg/L as $CaCO_3$. The high bound alkalinity is possibly an overestimate; at such elevated levels of dissolved carbonate, degassing of CO_2 to pore space in overlying unsaturated materials could be expected.

[4] Groundwater often contains high levels of dissolved CO_2. In contact with air, CO_2 would be expected to degas until equilibrium with air is attained.

- Trends in concentration ranges for seepage/groundwater mixtures often simply reflect the degree of dilution with groundwater. Some influence from secondary mineral precipitation is evident for Al, Fe and Zn; however, the effect on dissolved concentrations is relatively minor. Secondary mineral stability is also predicted to affect dissolved concentrations of Cu, Pb and Mn, due to langite, cerussite and rhodochrosite precipitation (Table 6.2 and Table 6.3).

Figure 6.2: Groundwater composition as a function of mixing proportions with LST seepage (base case conditions, maximum seepage concentrations)

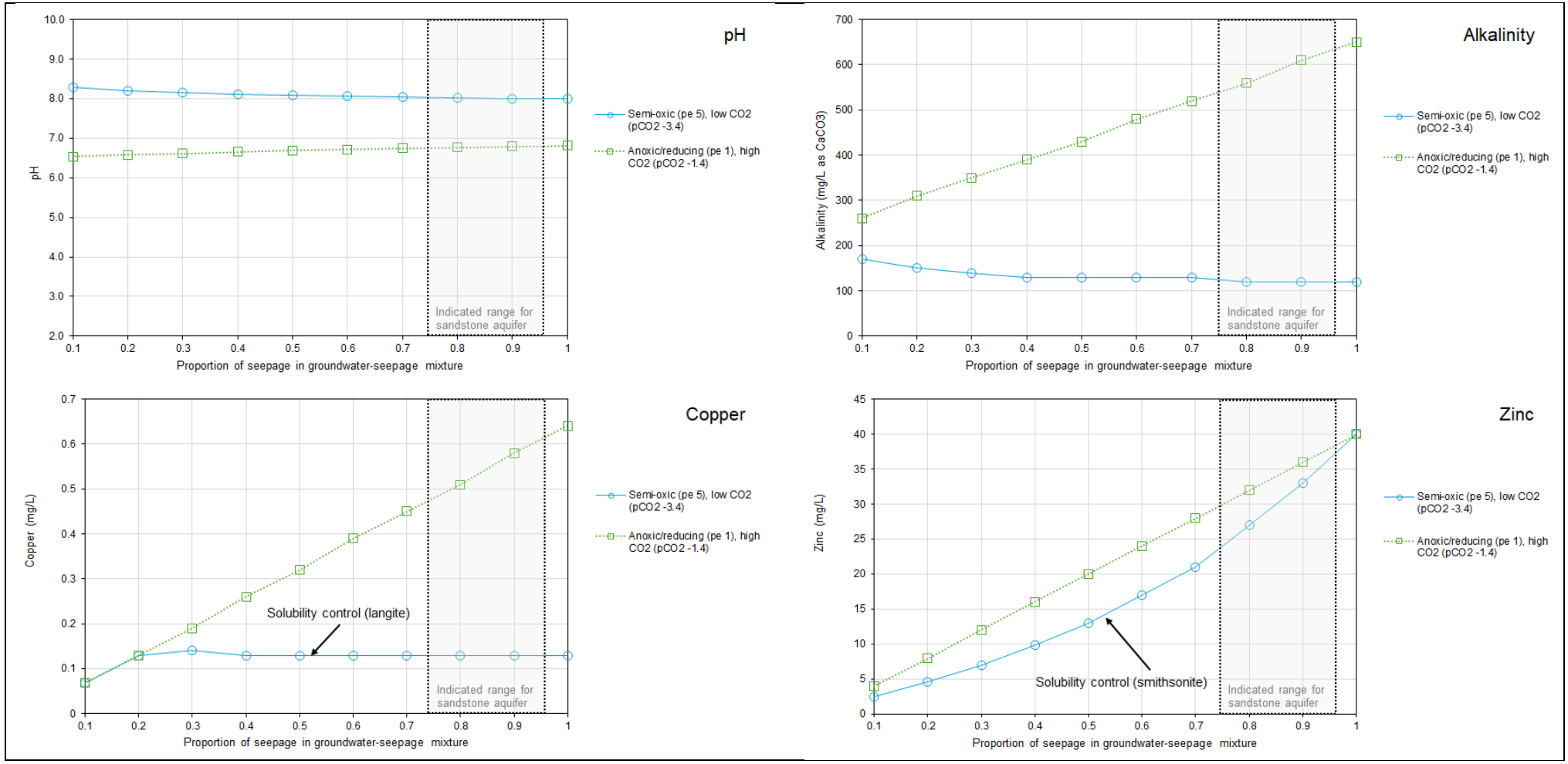

Notes: Simulations presented in the figures reflect (i) anoxic groundwater (Eh ~60 mV) with highly elevated CO_2 (4%v/v) and semi-oxic (Eh ~300 mV) with CO_2 at atmospheric concentrations (0.04 %v/v).

Table 6.2: Calculated seepage and shallow aquifer groundwater mixture – LST seepage (base case conditions; 1% infiltration)

Parameter	Units	Sandstone aquifer groundwater	Proportion of seepage in seepage/groundwater mixture					
			0.1	0.3	0.5	0.7	0.9	1
pH	s.u	7.4	7.5	7.6	7.6	7.5	7.5	7.5
Total alkalinity	mg/L as $CaCO_3$	110	260	340	360	340	330	330
TDS	mg/L	-	1,800	5,100	8,100	11,000	14,000	16,000
Ca	mg/L	17	55	130	210	280	360	390
Mg	mg/L	8	230	680	1100	1500	2000	2200
Na	mg/L	120	150	200	250	310	360	390
K	mg/L	8	68	190	310	430	550	610
SO_4	mg/L	28	1200	3700	6100	8500	11000	12000
Cl	mg/L	120	120	110	100	99	92	89
F	mg/L	0.5	0.59	0.78	0.96	1.1	1.3	1.4
Al	mg/L	0.03	0.00017	0.00021	0.00021	0.0002	0.00019	0.00018
Sb	mg/L	0.0002	0.0002	0.0002	0.0002	0.0002	0.0002	0.0002
As	mg/L	0.003	0.003	0.003	0.003	0.003	0.003	0.003
Ba	mg/L	0.16	0.0067	0.0041	0.0033	0.0029	0.0025	0.0024
Be	mg/L	0.0001	0.039	0.12	0.19	0.27	0.35	0.39
B	mg/L	0.24	0.24	0.24	0.24	0.24	0.24	0.24
Cd	mg/L	0.0001	0.039	0.12	0.19	0.27	0.35	0.39
Cr	mg/L	0.001	0.48	1.4	2.4	3.3	4.3	4.8
Co	mg/L	0.0001	4.3	13	21	30	38	43
Cu	mg/L	0.004	0.068	0.19	0.32	0.45	0.58	0.63
Fe	mg/L	0.2	0.0001	0.000098	0.0001	0.00011	0.00012	0.00013
Pb	mg/L	0.0003	0.023	0.067	0.11	0.15	0.19	0.22
Li	mg/L	0.0051	0.35	1	1.7	2.4	3.1	3.5
Mn	mg/L	0.11	0.86	2.1	3	4.6	6.5	7.6
Mo	mg/L	0.0055	0.0055	0.0055	0.0055	0.0056	0.0056	0.0056
Ni	mg/L	0.002	4.3	13	21	30	38	43
Se	mg/L	0.00025	0.00025	0.00025	0.00025	0.00025	0.00025	0.00025
Si	mg/L	28	7.9	7.8	7.7	6.4	4.5	3.6
Ag	mg/L	0.00001	0.00001	0.00001	0.00001	0.00001	0.00001	0.00001
Sr	mg/L	0.29	0.55	1.1	1.6	2.1	2.6	2.8
Tl	mg/L	0.00002	0.00002	0.00002	0.00002	0.00002	0.00002	0.00002
Sn	mg/L	0.0003	0.0003	0.0003	0.0003	0.0003	0.0003	0.0003
U	mg/L	0.00018	0.16	0.49	0.81	1.1	1.5	1.6
V	mg/L	0.0012	0.0012	0.0012	0.0012	0.0012	0.0012	0.0012
Zn	mg/L	0.009	4	9	13	21	33	40
Secondary mineral controls			Barite, chalcedony, diaspore, ferrihydrite	Barite, chalcedony, diaspore, ferrihydrite rhodochrosite, smithsonite	Barite, chalcedony, diaspore, magnesite, ferrihydrite rhodochrosite, smithsonite	Barite, cerussite, diaspore, magnesite, ferrihydrite rhodochrosite, smithsonite	Barite, cerussite, diaspore, magnesite, ferrihydrite, rhodochrosite, smithsonite	Barite, cerussite, magnesite, ferrihydrite, gypsum, langite, rhodochrosite

Notes: Values presented in the table reflect intermediate geochemical conditions (partial pressure CO_2 – 0.3%v/v; Eh - ~300 mV) consistent with semi-oxic groundwater and elevated CO_2 (10 × atmospheric levels).

Table 6.3: Calculated seepage and shallow aquifer groundwater mixture – LST seepage (sensitivity case; 9% infiltration)

Parameter	Units	Sandstone aquifer groundwater	Proportion of seepage in seepage/groundwater mixture					
			0.1	0.3	0.5	0.7	0.9	1
pH	s.u	7.4	7.5	7.5	7.6	7.6	7.6	7.6
Total alkalinity	mg/L as $CaCO_3$	110	240	280	310	330	360	370
TDS	mg/L	-	990	2300	3700	5000	6400	7000
Ca	mg/L	17	63	150	250	340	430	470
Mg	mg/L	8	88	250	410	570	730	810
Na	mg/L	120	120	130	130	130	140	140
K	mg/L	8	29	72	110	160	200	220
SO_4	mg/L	28	560	1600	2700	3700	4800	5300
Cl	mg/L	120	110	94	77	59	42	33
F	mg/L	0.5	0.5	0.51	0.52	0.53	0.54	0.54
Al	mg/L	0.03	0.00016	0.00018	0.00019	0.0002	0.00022	0.00013
Sb	mg/L	0.0002	0.0002	0.0002	0.0002	0.0002	0.0002	0.0002
As	mg/L	0.003	0.003	0.003	0.003	0.003	0.003	0.003
Ba	mg/L	0.16	0.01	0.0058	0.0046	0.004	0.0036	0.0035
Be	mg/L	0.0001	0.014	0.042	0.071	0.099	0.13	0.14
B	mg/L	0.24	0.24	0.24	0.24	0.24	0.24	0.24
Cd	mg/L	0.0001	0.014	0.042	0.071	0.099	0.13	0.14
Cr	mg/L	0.001	0.18	0.54	0.91	1.3	1.6	1.8
Co	mg/L	0.0001	1.6	4.8	8.1	11	15	16
Cu	mg/L	0.004	0.069	0.2	0.33	0.46	0.59	0.65
Fe	mg/L	0.2	0.0001	0.0001	0.0001	0.0001	0.000098	0.000098
Pb	mg/L	0.0003	0.018	0.055	0.091	0.095	0.099	0.1
Li	mg/L	0.0051	0.14	0.4	0.66	0.92	1.2	1.3
Mn	mg/L	0.11	0.78	1.6	1.9	2.2	2.3	2.4
Mo	mg/L	0.0055	0.0055	0.0055	0.0055	0.0055	0.0055	0.0055
Ni	mg/L	0.002	1.6	4.8	8.1	11	15	16
Se	mg/L	0.00025	0.00025	0.00025	0.00025	0.00025	0.00025	0.00025
Si	mg/L	28	7.9	7.9	7.8	6.5	4.6	3.6
Ag	mg/L	0.00001	0.00001	0.00001	0.00001	0.00001	0.00001	0.00001
Sr	mg/L	0.29	0.36	0.51	0.65	0.79	0.94	1
Tl	mg/L	0.00002	0.00002	0.00002	0.00002	0.00002	0.00002	0.00002
Sn	mg/L	0.0003	0.0003	0.0003	0.0003	0.0003	0.0003	0.0003
U	mg/L	0.00018	0.063	0.19	0.31	0.44	0.56	0.62
V	mg/L	0.0012	0.0012	0.0012	0.0012	0.0012	0.0012	0.0012
Zn	mg/L	0.009	2.9	7.3	8.5	9.5	10	11
Secondary mineral controls			Barite, chalcedony, diaspore, ferrihydrite	Barite, chalcedony, diaspore, ferrihydrite, rhodochrosite, smithsonite	Barite, cerussite, chalcedony, diaspore, ferrihydrite, rhodochrosite, smithsonite	Barite, cerussite, diaspore, ferrihydrite, rhodochrosite, smithsonite	Barite, cerussite, diaspore, ferrihydrite, rhodochrosite, smithsonite	Barite, cerussite, ferrihydrite, gypsum, langite, rhodochrosite, smithsonite

Notes: Values presented in the table reflect intermediate geochemical conditions (partial pressure CO_2 – 0.3%v/v; Eh – ~300 mV) consistent with semi-oxic groundwater and elevated CO_2 (10 × atmospheric levels).

It could be expected that there would be some mixing of seepage from the LST and HST cells along percolation pathways from the base of the TSF to the groundwater table. Further mixing could be expected as the seepage mixes with groundwater beneath the TSF footprint. As discussed in Section 5.2, development of acidic conditions in HST seepage (in the long term) cannot be precluded. Both the LST seepage and baseline groundwater are expected to contain alkalinity, as will HST seepage during drain-down.

The TSF system as a whole is expected to evolve through several phases:

- Drain-down – excess process water draining from TSF cells.
- Transitional – residual process water is being displaced by infiltrating meteoric water. Oxidation is taking place in the near-surface tailings, and percolates contain leachable oxidation products.
- Long-term – influence from near-surface sulfide oxidation has arrived at base of TSF cells and seepage is now dominated by the influence of oxidation.

The onset and duration of these phases differs between the LST and HST cells. For example, drain-down from the LST cells is expected to be complete in 5 to 10 years. In the case of the HST cells, engineering designs are expected to inhibit drain-down. Estimates for eventual drain-down (i.e. replacement of process water stored in pore space) are of order 600 to 3,500 years (Section 5.2.1).

Figure 6.3 is a schematic illustrating the acid-base balances that could apply at different stages in the evolution of seepage from the TSF (base case).

The following assumptions apply:

- Low bound LST alkalinity is assumed equal to groundwater. Higher bound is guided by estimated seepage composition in current study (Table 5.3) and controlled by carbonate-based neutralisation processes within the TSF.
- LST seepage will continue to contain alkalinity in the long term, at levels assumed to be equivalent to groundwater. There is uncertainty as to the process that might influence alkalinity within LST seepage during this period (carbonates may have leached from the tailings profile).
- During drain-down, HST seepage contains alkalinity (based on process water composition, Table 2.5). Following drain-down, HST seepage may contain acidity; the acidity range adopted was guided by values reported for synthetic AMD (Rio Tinto 2024b).
- Flux estimates were guided by values presented in Table 6.1.

Based on the information presented in Figure 6.3, acid-base balances suggest that mixed seepage would remain circumneutral during the prolonged drain-down period for the HST. During the transitional period, there is uncertainty as to the acid-base balance ranges from excess alkalinity to excess acidity.

Figure 6.3: Estimated acid-base balance in mixed flows of seepage and groundwater (base case conditions)

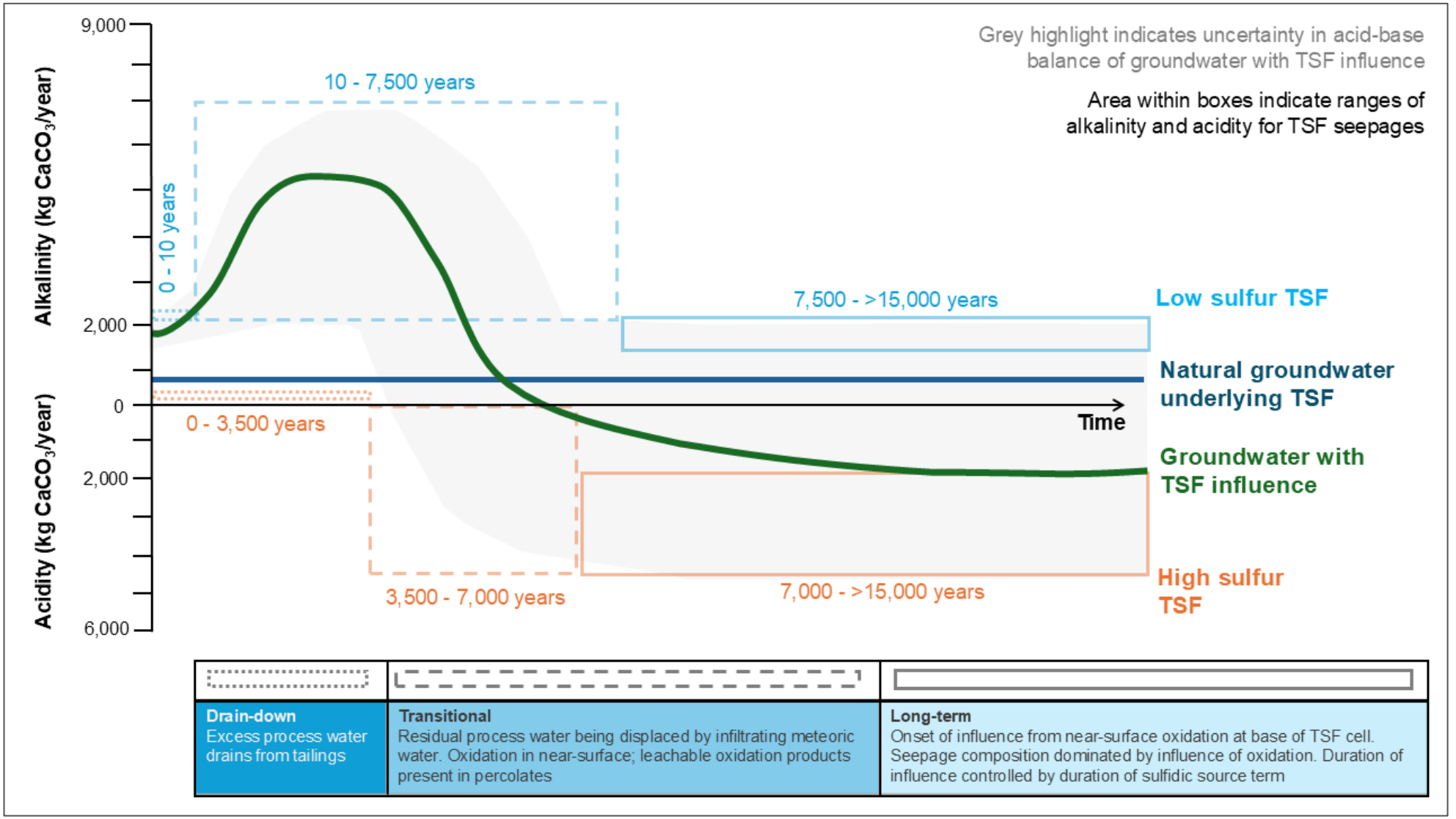

Notes: Prepared using flux estimates presented in Table 6.1.

6.3 Potential impacts to pit lake water quality

The Winu pit lake water quality model (HydroGeoLogica, 2024) indicates that the future lake, a terminal hydraulic sink, will be non-acidic with concentrations of metals/metalloids and salts that will continue to increase due to evapoconcentration until solubility limits are reached. Given model assumptions, the future lake can therefore be characterised as 'saline, circumneutral and metalliferous'.

Potential impacts to pit water quality from TSF seepage, in the context of current predictions, can be summarised as follows:

- Short-term impacts (within 300 years of closure): No impacts to pit lake water quality are expected within 300 years of closure. The range of seepage percolation and groundwater flow rates considered indicates that seepage-affected groundwater is unlikely to daylight in the pit void within 300 years.
- Long-term impacts (several hundred to thousands of years):
  - Initial phases of LST and HST seepage would resemble process water, which is indicated to be near neutral with net alkalinity. Indicative concentrations of some solutes in process water, are elevated with respect to pre-mining groundwater quality: SO_4, Cd, Co, Cu, Mn, Mo, Ni, Pb, Sb, Se, Tl and U. These 'sulfide-associated' solutes are inferred to reflect partial oxidation of the tailings during processing.
  - Subsequent phases of LST and HST seepage would be more strongly influenced by sulfide oxidation, further increasing concentrations of sulfide-associated solutes in groundwater relative to initial phases. Base and sensitivity model cases indicate that LST seepage will remain circumneutral, and that HST seepage may also remain non-acidic. Therefore, the characterisation of future pit water quality (saline, circumneutral and metalliferous) is unlikely to materially change due to inflows of seepage-affected groundwater over long timeframes.
  - On a multi-millennial timescale, generation of net acidity in seepage from HST cells cannot be precluded. However, given the timeframes involved, there is a high level of uncertainty around potential for net acid conditions in seepage-affected groundwater and potential influences on pit lake water quality.

7 Conclusions

The findings from this assessment can be summarised as follows:

- The slow rates of infiltration and seepage from the TSF (LST and HST cells) suggest that extremely long timeframes (many centuries, even millennia) would elapse before seepage would reach and mix with groundwater beneath the TSF.
- Seepage-affected groundwater is unlikely to report to the pit lake within the 300-year projection period of the pit lake model. The lag time for seepage-affected groundwater to daylight in the pit void would depend on the transport pathway (i.e. via aeolian sands or sandstone aquifer), relevant hydraulic conductivity, topography of aquifer-aquitard contacts and hydraulic gradient. Estimates of travel times to the pit vary widely, from around 150 years (more rapid transport in aeolian sands) to 13,000 years (sandstone aquifer).
- Initial phases of seepage will resemble process water (drain-down phase). Process water (LST and HST) is expected to be near-neutral, with dissolved concentrations of some metal(loid)s that could be slightly elevated compared to typical groundwater. LST cells are expected to drain-down over a 5–10-year period. For the HST cells, closure designs are expected to limit the rates of desaturation and drain-down. Estimates for eventual drain-down are of the order of 600 to 3,500 years.
- Following drain-down there will be a transitional phase while any residual process water is displaced by infiltrating meteoric water. Oxidation is taking place in the near-surface tailings, and percolates may contain leachable oxidation products. The duration of the transitional phase could be expected to reflect the duration of 1–2 pore volume exchanges through the tailings cells (i.e. order of 800–7,500 years for the LST, and 600–3,500 years for the HST). In the longer term, seepage would be strongly influenced by oxidation of sulfides present in unsaturated tailings.
- The onset and duration of seepage phases differs significantly between the LST and HST cells:
  - LST cells are expected to drain-down relatively rapidly, after which oxidation related processes could be expected to influence seepage composition. Slow net percolation rates suggest that basal seepage would not exhibit strong oxidation-related trends until a long time has elapsed (many centuries).
  - For HST, the drain-down period would be extremely long, and oxidation could be constrained to thin unsaturated layers near the cover interface for many millennia (to timeframes beyond the confidence limits of model simulations).
- So that potential long-term influences could be assessed in the case of the LST, the current study included modelling of basal TSF seepage composition, accounting for rates of sulfide oxidation over time, concomitant solute release, water-mineral interactions and elution from the tailings bed. The modelling showed that:
  - solute release profiles were strongly affected by the relationship between sulfide oxidation (and solute production) rates and the assumed net percolation rate.
  - circumneutral pH conditions are expected based on the overall acid-base balance within the tailings solid.

  - mineral solubility controls would place upper bounds in seepage concentrations of many parameters – e.g. sulfate, Al, Ba, Cu, Fe, Mn, Pb, Zn.

- Groundwater flux within aquifers beneath the TSF is low and, when compared to the large TSF footprint, may offer limited dilution capacity. Groundwater flowing between the TSF footprint and the pit may therefore contain relatively high proportions of TSF seepage, between 0.75 and 0.95 for LST, and between 0.4 and 0.8 for HST.

Closure

This report, Tailings Storage Facility Seepage Modelling, was prepared by

Thomas Robson, PhD
Senior Consultant (Geochemistry)

and reviewed by

Claire Linklater, PhD
Principal Consultant (Geochemistry)

All data used as source material plus the text, tables, figures, and attachments of this document have been reviewed and prepared in accordance with generally accepted professional engineering and environmental practices.

References

Advisian, 2022. Winu dewatering strategy and groundwater supply update, memorandum 311012-01475-5.1.1-TM-001-Rev0, 14 October 2022.

Advisian, 2023. Winu Gold and Copper Project: Infiltration Pond Study. Technical report prepared by Avisian Pty Ltd (Advisian) for Rio Tinto.

Alakangas, L, Lundberg, A and Öhlander, B, 2008. Pilot-scale Studies of Different Covers on Unoxidised Sulphide-rich tailings, Northern Sweden: Oxygen Diffusion, in *Mine Water and the Environment* (eds: N Rapantova and Z Hrkal), pp 347–350 (VSB – Technical University of Ostrava: Ostrava).

Demers, I, Bussière, B, Mbonimpa, M and Benzaazoua, M, 2009. Oxygen diffusion and consumption in low-sulphide tailings covers, *Canadian Geotechnical Journal*, 46(4):454–69. https://doi.org/10.1139/T08-132.

Garvie, A M, Linklater, C M, Chapman, J T and Watson, A, 2014. Overall acid production rates in mine wastes, in *Proceedings of the 8th Australian Workshop on Acid and Metalliferous Drainage*, Adelaide, South Australia 29 April – 2 May 2014 (eds: H Miller and L Preuss), pp 111–124 (JKTech Pty Ltd: Brisbane).

Golder, 2022. H3 Hydrogeological Assessment of the Winu Project. 20136763-062-R-Rev3. March 2022. Prepared for Rio Tinto Copper by Golder Associates Pty Ltd (Golder).

Green, R, personal communication (email 9 October 2024).

HydroGeoLogica, 2024. Winu pit lake model, Draft 2, dated May 2024. Prepared for Rio Tinto Winu Pty Ltd by HydroGeoLogica Inc (CO, USA).

INAP (International Network for Acid Prevention), 2009. Global Acid Rock Drainage Guide (GARD Guide). gardguide.com.

Nordstrom, D K and Alpers, C N, 1999. Geochemistry of Acid Mine Waters, in *The Environmental Geochemistry of Mineral Deposits, Part A: Processes, Techniques, and Health Issues* (eds: G S Plumlee and M J Logsdon) Reviews in Economic Geology Volume 6A, pp 133–160 (Society of Economic Geologists Inc: Littleton).

O'Kane, 2020. Winu copper project – Conceptual cover system modelling, Report 0662-049-001. Technical report prepared for Rio Tinto by Okane Consultants Pty Ltd.

O'Kane, 2024. Winu updated tailings storage facility cover system numerical modelling, Report 0662-272-002, May 2024. Technical report prepared for Rio Tinto by Okane Consultants Pty Ltd.

Parkhurst, D L and Appelo, C A J, 2013. Description of input and examples for PHREEQC version 3 – A computer program for speciation, batch-reaction, one-dimensional transport, and inverse geochemical calculations: U.S. Geological Survey Techniques and Methods, book 6, chap. A43, 497 p., https://doi.org/10.3133/tm6A43

Ritchie, A I M, 1995. Application of oxidation rates in rehabilitation design, in *Proceedings of the Second Australian Acid Mine Drainage Workshop* (eds: N J Grundon and L C Bell), pp 101–116 (Australian Centre for Minesite Rehabilitation Research: Brisbane).

Rio Tinto, 2024a. Winu project: Conceptual Mine Closure Plan, dated 31 January 2024.

Rio Tinto, 2024b. Winu waste characterisation – Tailings, Version 3 report, dated 20 June 2024.

SRK, 2020. Winu Study – Oxidation Rate Assessment. Report prepared for Rio Tinto Copper and Diamonds by SRK Consulting (Australasia) Pty Ltd. Project RTS198. September 2020.

Vincent, M, Aubertin, M, Bussière, B, Mbonimpa, M, Dagenais, A and Gosselin, M, 2006. Measurement of oxygen consumption and diffusion in exposed and covered reactive mine tailings, J*ournal American Society of Mining and Reclamation*, 2006(2):1156–69. https://doi.org/10.21000/JASMR06021156.

Worley, 2024a. Winu H3 Hydrogeological assessment: 2024 Update, Doc Rev B: REP-HG-025, 9 June 2024.

Worley, 2024b. H3 Hydrogeological assessment: Winu project area, Doc Rev B: REP-HG-032, 29 July 2024.

WWL, 2024a. Winu HDTSF 5H Pre-feasibility Design Report, prepared for Rio Tinto by Water, Waste and Land Consulting Engineers and Scientists, Perth, Report No. 127-032-1, 10 June.

WWL, 2024b. Winu TSF Closure Design. Prepared for Rio Tinto by Water, Waste and Land Consulting Engineers and Scientists, Perth. Report No. 127-029-1-RevC, 6 December.

WWL, 2024c. Winu HDTSF Seepage Modelling. Prepared by Water, Waste and Land Consulting Engineers and Scientists for Rio Tinto, Report No. 127-029-Appendix C, September 2024.

WWL, 2024d. Winu Copper - Closure Design of TSFs. Tailings Storage Facilities Basis of Design: Closure Design. Prepared by Water, Waste and Land Consulting Engineers and Scientists for Rio Tinto, Report No. MEM-C0007-B013-WWL-MEM-00013.00-Appendix A, July 2024.